ISSN 0140 3818
SSSU 3/77

UNIVERSITY OF SOUTHAMPTON

DEPARTMENT OF SHIP SCIENCE

FACULTY OF ENGINEERING AND APPLIED SCIENCE

THE FREE-STREAM CHARACTERISTICS OF A SEMI-BALANCED SHIP SKEG-RUDDER

by A.F. Molland

Ship Science Report No 3/77

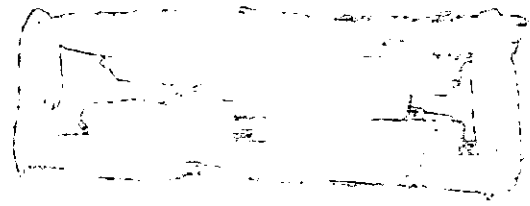

THE FREE-STREAM CHARACTERISTICS OF A SEMI-BALANCED SHIP SKEG-RUDDER

A. F. Molland

May 1977

SUMMARY

The results of free-stream wind tunnel experiments on a semi-balanced skeg rudder are presented.

The tests on this rudder, which has skeg and overall characteristics which are typical for the rudders fitted to many modern ship types, are the first in a projected series of tests on skeg rudders.

The experiments establish a better understanding of the working and performance of the semi-balanced skeg rudder, and provide design data. Results are presented as lift, drag and normal force coefficients and centre of pressure for the rudder plus skeg combination, for the rudder alone and skeg alone; a complete range of rudder angle of attack was tested for selected positive and negative angles of attack on the skeg.

In order to provide a basis for comparison, the all-movable rudder case was simulated by sealing the gap between rudder and skeg. The results for the all-movable case compare very satisfactorily with existing published data, thus confirming the satisfactory operation of the new dynamometer, instrumentation, test techniques and analysis.

The results for the skeg rudder show that, with increasing angle of attack, discontinuities occur in the growth of lift together with a large movement of centre of pressure. The skeg rudder results are compared with those for the all-movable case, and the flow breakdown accounting for the discontinuities in the skeg rudder characteristics is discussed.

Visual flow studies with supporting photographs are described; these are in general agreement with the flow breakdown indicated by the force measurements.

CONTENTS

1. INTRODUCTION

A fundamental approach to the design of ship rudders is being used increasingly by designers; namely, the free-stream or open-water characteristics for a suitable rudder are used, together with a velocity and angle of attack to which modifying factors have been applied. The rudder in the free-stream condition and the modifying effects on the free-stream of the hull and propeller are, therefore, treated as individual components of the complete system.

Current deficiencies in the method are known to exist, and these include the derivation or availability of suitable modifying factors for the widely varying effects of hull and propeller and, the availability of suitable free-stream data for particular rudder types.

Such a breakdown into components does, however, have the important merit that it allows free-stream investigations to be made of the variation in rudder forces, due to changes in rudder parameters, which are independent of the effects of different hull forms and propeller arrangements.

This design procedure basically requires the use of free-stream or open-water data applicable to ship rudder configurations. Recourse has been made by the designer to relatively large quantities of published aerodynamic free-stream data; the principal data available are for symmetrical section aerofoils of low aspect ratio, and are suitable for many ship applications, e.g. Refs.1 and 2. Less information is available for flapped control surfaces suitable for ship applications, e.g. Refs.3 and 4.

Referring to more recent developments in ship rudder types, the semi-balanced rudder supported by a fixed horn or skeg is being increasingly fitted to vessels of all types. Whilst the skeg rudder is a combination of all-movable and flapped rudders, it does not necessarily follow that the characteristics of the skeg rudder are intermediate between the all-movable and flapped rudder; this point was discussed, for example, in Ref.5. Whilst some experiments on semi-balanced rudders are reported in Ref.6 and isolated free-stream tests on a skeg rudder are

included in Ref.7, comprehensive free-stream information on such rudders is very limited and no systemmatic studies are known to have been carried out; the need for more data on this type of rudder was also discussed in Ref.8.

In view of the increasing application of the semi-balanced skeg rudder, an investigation into the free-stream characteristics of this rudder type was initiated.

In the normal way, for a given velocity and angle of attack, a knowledge of the forces and moments acting on the rudder and skeg (both separately and combined) is required in order to compute:

(a) the rudder torque, necessary in the design of rudder stock and steering gear,

(b) the moments about root of rudder, necessary for structural design considerations and

(c) the lateral force acting on the ship, necessary in the determination of manoeuvring characteristics.

In order to minimise scale effects, it was desirable that the projected tests be carried out in a wind tunnel where a high Reynolds Number could be achieved; various sources suggest that trustworthy results should be obtained when the Reynolds Number is upward of 1,000,000. Further, in order to derive the necessary forces and moments at various angles of attack for both rudder and skeg, a new wind tunnel dynamometer was required to be designed and constructed specifically for this purpose.

Tests on a series of rudders are projected, and this Report describes and discusses the results for the first rudder which has skeg and overall characteristics which are typical for the rudders fitted to many modern ship types.

2. DESCRIPTION OF MODEL

The model was lamenated from jelutong with a mean geometric chord $\bar{c}$ of 457 mm. This value was chosen as being the largest size possible commensurate with acceptable limits on corrections due to wall effects.

The principal characteristics of the rudder are as follows:-

Mean Chord	$\bar{c}$	=	457 mm
Span	S	=	680 mm
Geometric Aspect Ratio	AR_G	=	1.49
Taper Ratio	C_T / C_R	=	0.59
Thickness/Chord Ratio	t/c	=	0.20
Section		=	NACA 0020 Root and Tip, with square tip
Sweep of Quarter Chord	Ω	=	3.8°
Skeg Depth/Span		=	0.50
Skeg Area Ratio		=	20.5%
Balance Area Ratio		=	19%
Horizontal and Vertical Gaps Between Skeg and Rudder		=	4 mm

In way of the skeg the overall NACA 0020 section shape was maintained for the rudder plus skeg combination; the nose radius of the portion of movable rudder behind the skeg was approximately one-half the local section thickness at the centreline of stock. Further particulars of the rudder are given in Fig.1, and more detailed reasons for the choice of the model rudder characteristics are given in APPENDIX A1.

Leading edge roughness (a turbulence strip) was applied to both sides of the rudder, and consisted of 0.0059 in Dia. carborundum grit (No.100) spread evenly over double-sided adhesive tape of 10 mm width; the leading edge of the roughness strip was located 5% aft of the leading edge of the chord.

3. APPARATUS AND TESTS

The tests were carried out in the 7" x 5" low-speed wind tunnel at Southampton University, Ref.9.

The rudder was mounted through the tunnel floor and the gap between the rudder and the floor was approximately 2.5 mm (0.0055 $\bar{c}$).

Force and Moment measurements were made using the strain-gauge dynamometer described in Ref.10; this dynamometer is capable of the measurment of five components leading to the derivation of lift, drag and centre of pressure chordwise and spanwise, can measure the rudder and skeg forces either separately or combined and allows independent adjustment of angle of attack for both rudder and skeg about a common axis. The accuracy of the dynamometer is within $\pm$ 1.2% for torque and within $\pm$ 0.4% for the remaining components.

Fig. 2a shows a photograph of the skeg rudder in the wind tunnel, and Fig. 2b gives a similar view but with floor removed to show the dynamometer.

The tests were carried out at dynamic pressures of 0.1194 m and 0.0584 m of water, which correspond to nominal wind speeds of 46 m/s and 32 m/s and nominal Reynolds Numbers of 1.23×10^6 and 0.86×10^6 at the mean test temperature of 38°C and mean pressure of 102×10^3 N/m^2 .

Tests were carried out in the ahead condition for variation in the rudder angle of attack δ , in $2\frac{1}{2}^\circ$ increments, over a range of angles up to stall; this range of tests was carried out for fixed values of skeg angle β of approximately -15°, -10°, -5°, 0°, 5°, 10°, 15°. All the basic tests were carried out at a nominal Reynolds Number of 1.23×10^6 ; in order to determine the influence of Reynolds Number, some extra tests were carried out at a nominal Reynolds Number of 0.86×10^6 .

One test condition ($\beta = 0$) was repeated with the leading edge roughness removed.

Tuft studies were carried out in order to observe the flow over the rudder; white wool tufts, approximately 25 mm long, were attached to the rudder with clear adhesive tape and photographs taken of the results for both sides of the rudder at various angles of attack. (Leading edge roughness, as for the force measurements, was applied for the tuft studies).

Finally, in order to provide a basis for comparison with the skeg rudder, and to provide a comparison with existing published all-movable data, tests were carried out on a simulated all-movable rudder of the same dimensions as the rudder plus skeg combination; this was achieved by sealing the gap between the rudder and skeg with plasticine and black adhesive tape, and varying the angles of attack of rudder and skeg simultaneously. Leading edge roughness was applied for this simulated all-movable case.

4. DATA REDUCTION AND CORRECTIONS

A computer program was written, Ref.11, to provide the final data in coefficient form; the program incorporates the dynamometer five-component interaction matrix and correction formulae, the resolution of forces and moments from instrument axes to stream axes as necessary, and includes corrections for wind tunnel boundary effects.

The raw data was zero corrected before insertion in analysis program; a cross plot of zero-corrected raw data yielded the angular misalignment in the rig which amounted to 0.25° and this correction was applied to all measured angles before insertion in the program.

Tunnel boundary corrections were applied as described in Ref.12 and outlined in Ref.11 and amounted to corrections due to solid blocking, streamline curvature and downwash. The net corrections for this rudder are summarised as follows:

$$C_{Lc} = 0.9956\ C_{Lu}$$

$$\alpha_c = \alpha_u + 0.7706\ C_{Lu}$$

$$C_{Dc} = 0.9956\ C_{Du} + 0.0110\ C_{Lc}^2$$

where suffixes 'u' and 'c' indicate the uncorrected and corrected values respectively.

The boundary correction to rudder angle α is not applied to the skeg angle β ; this correction varies typically from zero up to about 0.7° at maximum rudder angle and, without cross-fairing, its application would not allow direct comparison between results for different fixed values of β for variation in rudder angle.

5. PRESENTATION OF DATA

The notation of the angles and coefficients used in the presentation is given in Fig.3.

The results of the tests are tabulated in non-dimensional form in APPENDIX A3 and are presented graphically in Figs.4 to 10. These plots show force coefficients, centre of pressure chordwise (as a percentage of mean chord from leading edge) and centre of pressure spanwise (as a percentage of span from root) versus angle of attack. In the test results, the total area of rudder plus skeg is also used in deriving the force coefficients for rudder alone and skeg alone; this allows direct comparisons to be made between the absolute forces on the rudder, skeg and rudder plus skeg. The only exception to this is in the graphical presentation of normal force coefficient C_N for rudder alone, described below.

Fig.4 shows the results for the all-movable rudder plotted to a base of α, the rudder angle relative to the wind.

In Figs. 5a to 5g the results for both rudder plus skeg and rudder alone are plotted to a base of α, the angle of rudder relative to wind, for various fixed values of skeg angle β.

In Fig.6 the lift characteristics for the rudder alone for selected skeg angles are reproduced.

Fig.7 shows the lift characteristics for the skeg alone, plotted to a base of α.

In Fig.8 a comparison is made between lift coefficient versus angle of attack α for the all-movable case, rudder plus skeg for $\beta = 0$, rudder plus skeg for $\beta = 0$ at reduced Reynolds Number, and rudder plus skeg for $\beta = 0$ without transition strip.

In order to provide a direct comparison with the all-movable rudder, the corrections to the skeg rudder data necessary to yield the $\beta = 0$ case from the $\beta = -0.25^{\circ}$ case were carried out for the results shown in this diagram.

In Fig.9 the movable rudder normal force coefficient C_N curves based on movable area only, for various fixed values of skeg angle β, are plotted to a base of δ, the angle of the rudder relative to the skeg (or ship). Whilst for consistency the test results for C_N are based on total area, for possible design applications the graphical presentation of C_N in Fig.9 is based on movable area; i.e. since for this rudder (skeg area/total area) = 0.205, the coefficients C_N in the tabulated test results have been divided by 0.795 in order to derive the coefficients based on movable area.

In Fig.10 the normal force coefficient C_Y curves based on total area of rudder plus skeg, for various fixed values of skeg angle β, are plotted to a base of δ, the angle of the rudder relative to the skeg (or ship).

Photographs of the tuft studies of flow patterns for a skeg angle β of -5° and various rudder angles δ, are shown in Fig.12.

6. DISCUSSION OF RESULTS

6.1 Comparison of All-Movable Rudder of Present Work with Existing Published Data:

The all-movable rudder forms a basis with which the skeg rudder can be compared. In order to check its characteristics, comparisons were made with the free-stream characteristics of all-movable control surfaces published by Whicker and Fehlner, Ref.2, and Jones, Ref.1.

Selected results of Refs.1 and 2 for a Reynolds Number of 0.86×10^6 and Geometric Aspect Ratio of 1.5, and corrected for sweep, thickness ratio and taper ratio as necessary, are reproduced below together with the results for the present work. The results for the present work for the complete range of rudder angles are shown in Fig.4.

	Ref.2. (Smooth)	Ref.1. (Smooth and L.E. Roughness)	Present Work (L.E. Roughness)
$\left[\frac{dC_L}{d\alpha}\right]_{\alpha=0}$	0.052	0.053 (Smooth) 0.051 (Rough)	0.048
$C_{L\,max}$	1.02	0.94 (Smooth) 0.77 (Rough)	0.91
α_{STALL}	22°	18°	20°
C_D @ 10°	0.043	-	0.040
C_D @ 20°	0.160	-	0.172
CP$\bar{c}$ @ 10°	18%	-	17.5%
CP$\bar{c}$ @ 20°	23%	-	23%
CPs @ 10°	45%	-	45%
CPs @ 20°	48%	-	47% just pre-stall

The results of Ref.1 with leading edge roughness would indicate a deficiency in the lift curve slope of the present work of approximately 0.002/degree. Further, tests in Ref.2 were carried out with a groundboard; making an approximate boundary layer displacement thickness correction (10 mm) to the present work would account for a further deficiency of approximately 0.001/degree. Taking into account the facts that the tests in Ref.2 were carried out with a groundboard displaced from the tunnel floor, tests in Ref.1 were carried out with a complete wing clear of tunnel walls, and that corrections for variation in the parameters of the various rudders are of necessity approximate, it is considered that the lift curve slope for the present work is very satisfactory.

The results of Ref.1 would indicate a decrease in $C_{L\,max}$ and a slightly earlier initiation of stall when leading edge roughness is applied. It is considered, therefore, that roughness probably accounts for the slightly lower values of $C_{L\,max}$ and α_{STALL} for the present work compared with Ref.2.

Considering the above qualifications concerning test conditions, drag coefficient and centre of pressure for the present work also show satisfactory agreement with Ref.2.

It is concluded that the overall characteristics of the all-movable rudder of the present work compare favourably with existing published data, and that its characteristics form a very satisfactory basis with which to compare the skeg rudder. The results also confirm the satisfactory operation of the new dynamometer and equipment which was constructed primarily for these tests.

6.2 Skeg Rudder Characteristics:

6.2.1 Lift and Stall

The lift characteristics for skeg angles varying from -15.25° to $+14.75^{\circ}$ are shown in Figs.5a to 5g. In all cases, including

the rudder plus skeg and rudder alone conditions, there is a distinct discontinuity in the growth of the lift curve. The discontinuity becomes more pronounced as negative angle of attack on the skeg is increased. The discontinuity is considered to be due to early separation aft of the skeg; flow through the gap between rudder and skeg is likely to be contributing to this early separation and this phenomenon, together with its influence on the characteristics of the skeg rudder, is the subject of a more detailed discussion later.

For all skeg angles the lift curve is approximately linear before and after the discontinuity, and of smaller slope after the discontinuity. Compared with a lift curve slope of 0.048/deg. for the all-movable rudder, the lift curve slope for the rudder plus skeg combination is approximately 0.038/deg. before the discontinuity for both negative and positive skeg angles; after the discontinuity it is approximately 0.029/deg. for negative skeg angles and approximately 0.022/deg. for positive skeg angles. Based on total area of rudder plus skeg (per Figs.5a to 5f) the lift curve slope of the rudder alone for all skeg angles is approximately 0.029/deg. before the discontinuity and 0.022/deg. after the discontinuity.

An inspection of the rudder alone curves indicates that the start of the decrease in rate of growth of lift occurs at about $\alpha = 7.5^\circ$ for the $\beta = -15.25^\circ$ case increasing to about $\alpha = 12.5^\circ$ for the $\beta = 9.75^\circ$ case. For comparative purposes the lift characteristics of rudder alone for $\beta = -10.25^\circ$, -0.25° and $\beta = +9.75^\circ$ are reproduced in Fig.6; the lift curve slopes and trends are seen to be similar. It is, however, interesting to note that at angles of attack up to about 10° the skeg angle of $\beta = -10.25^\circ$ produces a favourable inflow angle leading to an increase in lift compared with the $\beta = -0.25^\circ$ case, whilst the skeg angle of $\beta = +9.75$ is disadvantageous. As would be expected, once breakdown of flow occurs aft of the skeg, these conditions are reversed and more lift is produced by the $\beta = +9.75^\circ$ case.

Considering the $\beta = -0.25^\circ$ case (Fig.5d) after the discontinuity in lift curve it is seen that, of the total lift produced by the rudder plus skeg combination, about 83% of the lift is contributed by the movable portion of the rudder and the remainder by the skeg. The contribution of the skeg decreases with increase in negative skeg angle and

increases with increase in positive skeg angle.

Fig.7 shows the lift characteristics for the skeg alone. All the skeg angles show a similar trend; there is a steady build up of lift until separation aft of the skeg occurs at which stage there is a distinct decrease in the lift on the skeg. The decrease in the lift on the skeg is an indication of the influence of the flow leakage from the high pressure (face) side through the gap to the low pressure side. As rudder angle is further increased the positive and negative total pressure build up is such that the lift on the skeg starts to increase again.

A general observation from Figs.6 and 7 is that in relative terms the attitude of the skeg does not have a large effect on the lift produced by the movable portion of the rudder (Fig.6); a much greater proportion of the change in total lift of rudder plus skeg combination for variation in the skeg angle is due to the relatively larger change in the lift on the skeg itself (Fig.7).

Figs.5c to 5f indicate that the maximum lift coefficient $C_{L\,max}$ for rudder plus skeg combination (tested at a Rn of 1.23×10^6) varied from 1.010 for $\beta = 9.75^\circ$, 0.940 for $\beta = 4.75^\circ$, 0.870 for $\beta = -0.25^\circ$ to 0.850 for $\beta = -5.25^\circ$. ($C_{L\,max}$ was not attained for $\beta = 14.75^\circ$ due to vibrations in the rig, nor for $\beta = -15.25^\circ$ and -10.25° due to the limits of approximately 40° in angular adjustment of δ). The values compare with a $C_{L\,max}$ of 0.93 (corrected to a Rn of 1.23×10^6) for the all-movable rudder. Compared with the all-movable rudder, therefore, $C_{L\,max}$ for the rudder plus skeg combination is 1% larger for $\beta = 4.75^\circ$, 6% smaller for $\beta = -0.25^\circ$ and 9% smaller for $\beta = -5.25^\circ$.

Figs.5c to 5f show that the stall angle, α_{STALL}, for the rudder plus skeg was not influenced significantly by skeg angle and had values of 36°, 34°, 34° and 37° for skeg angles β of -5.25°, -0.25°, 4.75° and 9.75° respectively; α_{STALL} for the rudder alone was approximately 33° for each of the skeg angles. These values compare with a stall angle of 20° for the all-movable rudder.

Fig.8, which shows lift coefficient versus angle of attack for various conditions, includes the results for the all-movable rudder and the skeg rudder (for rudder plus skeg at $\beta = 0$); an overall picture of the differences in lift producing characteristics between the all-movable and skeg rudders is clearly seen.

6.2.2 Drag

An approximate comparison between the skeg rudder with $\beta = -0.25^{\circ}$ (Fig.5d) and the all-movable rudder (Fig.4) at zero angle of attack ($\alpha = 0$) indicates that C_{D_o} for the skeg rudder is up to about 10% greater than the all-movable rudder. A comparison in terms of equal lift shows that for lift coefficients of 0.250, 0.400 and 0.800 the drag of the skeg rudder is about 40% greater, 155% greater and 170% greater respectively. These differences in drag increase with increasing negative skeg angle and decrease a little with increasing positive skeg angle.

From Figs.5a to 5f it is seen that there is a discontinuity in the growth of drag with increase in angle of attack for both the rudder plus skeg and rudder alone cases; this discontinuity occurs approximately at the completion of separation and then stall of the portion of rudder behind the skeg.

Figs.5a to 5f also show that the drag of the rudder alone case is considerably lower than the case of rudder plus skeg for low angles of attack; close inspection in fact reveals that at low angles there is some negative (forward) drag on the rudder alone. This latter fact confirms that an attractive force existed between the rudder and skeg at low angles; using the case of $\beta = -0.25^{\circ}$ (Fig.5d) for discussion, as angle of attack is increased and the angle approached at which leakage through the gap would appear to commence (about $5^{\circ} - 7\frac{1}{2}^{\circ}$) the drag of the rudder alone is seen to increase relatively rapidly until it is, as would be expected, only a little less than the case of rudder plus skeg. If the rudder alone were treated as if in isolation, and without attraction, then if the total drag coefficient of 0.020 on the rudder plus skeg were assumed to be comprised of 0.004 due to friction and 0.016 due to form, and the movable part is assumed to account for, say, 80% (0.003) of the friction and 50% (0.008) of the form, then a drag coefficient of about 0.011 would have been expected from the movable part of the rudder.

The existence of an attractive force between rudder and skeg was not unknown nor unexpected; it has, for example, been described and discussed in Ref.4. The existence of this force does not invalidate the results of these tests for small angles; it should, however, be borne in mind that the

drag results for the rudder alone are not for the movable part in isolation but in association with a skeg having the overall properties and gap size used in these tests.

6.2.3 Centre of Pressure

Variation of centre of pressure, as a percentage of chord from leading edge and percentage of span from root, with angle of attack is shown plotted in Figs.5a to 5g. With positive lift on the movable rudder and negative lift on the skeg the true centre of pressure for the rudder plus skeg combination becomes indeterminate; the centre of pressure for rudder plus skeg has, therefore, been omitted for $\beta = -15.25^\circ$ and -10.25° in Figs.5a and 5b.

The centre of pressure chordwise, $\overline{CPc}$, for $\beta = -0.25^\circ$ is seen to have a relatively large amount of travel compared with the all-movable rudder (Fig.4); with increasing rudder angle, δ, $\overline{CPc}$ moves rapidly aft until separation behind the skeg is complete (approximately coincident with the discontinuity in the lift curve) after which the movement of $\overline{CPc}$ is less pronounced. A similar form of $\overline{CPc}$ travel is also indicated in the Report on tests carried out on semi-balanced rudders by Hagen, Ref.6. With increasing positive angle of attack β on skeg the movement of $\overline{CPc}$ is even more pronounced, whilst with increasing negative angle of attack its movement is less pronounced.

For skeg angles β between -10.25° and $+4.75^\circ$ the centre of pressure $\overline{CPc}$ for the rudder alone is seen to be forward of the rudder stock for rudder angle δ up to about $12\frac{1}{2}^\circ$, leading to negative torques. Published results, for example Refs.7 and 13, indicate that $\overline{CPc}$ is likely to be even further forward when working in a propeller slipstream, hence careful choice of balance area is required for this rudder type, particularly when working aft of a propeller, if negative torques are to be avoided.

Compared with the all-movable rudder the movement of the centre of pressure spanwise, CPs, is also seen to be relatively large for skeg angle $\beta = -0.25^\circ$, and for increasing negative and positive skeg angles. CPs for the rudder plus skeg combination is seen to be larger than that of the all-movable rudder; this is apparently due to the relatively larger proportion of the lift carried by the outboard 'all-movable' part of the skeg rudder after the portion aft of the skeg has stalled.

The centre of pressure of the skeg alone is included in the tabulated test results in APPENDIX A3; this data is, however, erratic, due mainly to the fact that the skeg centre of pressure position is analysed using the difference in forces on rudder plus skeg and rudder alone. When this difference tends to zero (such as when the lift curves cross for negative skeg angles) the data becomes irregular and unreliable.

6.2.4 Rudder Normal Force

The rudder normal force coefficient, C_N , (based on movable area) and chordwise centre of pressure characteristics for the rudder alone are shown plotted in Fig.9. This diagram gives an overall picture of the influence of skeg angle (or drift angle at rudder) on rudder normal force and centre of pressure. Since torque is defined as the rudder normal force times its distance from the rudder stock, the information contained in the diagram allows direct calculations for torque in the free stream condition to be made for a skeg rudder with the geometric properties the same as, or similar to, those outlined in Fig.1.

6.2.5 Ship Normal Force

The ship normal force coefficient, C_Y , characteristics for the rudder plus skeg combinations are shown plotted in Fig.10. This diagram gives an overall picture of the influence of skeg angle (or drift angle at rudder) on ship normal force due to the rudder. Use of the diagram, together with the appropriate centre of pressure from Figs.5c to 5g allows the calculation of the turning moment on the ship due to the rudder plus skeg combination in a free stream. Whilst the centre of pressure $\overline{CPc}$ of the rudder plus skeg combination for $\beta = -10.25^\circ$ and -15.25° were indeterminate, inspection of the data suggests that, compared with the distance of the rudder to the ship centre of gravity, the use of $\overline{CPc}$ for $\beta = -5.25^\circ$ for these cases would not incur significant error.

6.3 Visual Flow Studies:

Fig.12 presents photographs showing the results of the flow studies for a skeg angle $\beta = -5^\circ$ and a systemmatic variation in rudder angle δ . The photographs on the left hand side of the figure show the flow over the

back (low pressure) side of the rudder whilst the adjacent photographs on the right hand side of the figure show the flow over the face (high pressure) side for similar rudder and skeg angle conditions. The following general comments are given on the flow characteristics pertinent to the present study.

The photographs indicate that, on the back (low pressure) side, separation behind the skeg commences at about $\delta = 5^{\circ}$, has moved forward about half way along the movable portion by $\delta = 10^{\circ}$, and that the flow over the movable portion behind the skeg is completely separated at $\delta = 15^{\circ}$. The upper 'all-movable' portion is showing signs of separation at $\delta = 20^{\circ}$; this increases up through $\delta = 30^{\circ}$ until at $\delta = 40^{\circ}$ complete separation has occurred.

From the photographs of the face (high pressure) side, flow through the horizontal gap is seen to be starting at about $\delta = 10^{\circ}$ and is well established by $\delta = 15^{\circ}$. Reversal of one tuft into the vertical gap at $\delta = 15^{\circ}$ indicates the approximate start of a strong gap flow; by $\delta = 30^{\circ}$ most of the tufts are reversed into the gap.

Similar trends to those described above were recorded for skeg angles β of $+5^{\circ}$, 0° and $\pm 10^{\circ}$.

6.4 Separation and Gap Effect:

Discontinuities in the lift and drag curves, illustrated in Figs.55a to 55g, were described in SECTIONS 6.2.1 and 6.2.2 ; these discontinuities are evidently due to early separation behind the skeg; this early separation is confirmed by the visual flow studies, shown in Fig.12 and discussed in SECTION 6.3.

It was seen from the flow studies that whilst separation behind the skeg starts at relatively low rudder angles, separation on the 'all-movable" part of the rudder does not start until somewhat higher angles; hence an intermediate situation exists for the skeg rudder where the flow behind the skeg is fully separated whilst that clear of the skeg is still attached. This characteristic was reported in Ref.5, in which the confused flow was attributed to the horizontal break.

Flow through the vertical gap from high pressure side to low pressure side is evident from the visual studies; these studies suggest that strong gap flow may not be starting until the portion of the rudder behind the gap (skeg) is nearly completely separated (at about $\delta = 15^{\circ}$ or $\alpha = 10^{\circ}$ for the $\beta = -5^{\circ}$ case). The relatively rapid convergence of the drag results for rudder alone with those of rudder plus skeg at about $\alpha = 5^{\circ} - 7\frac{1}{2}^{\circ}$ for the $\beta = -0.25^{\circ}$ case (and similarly for the $\beta = -5.25^{\circ}$ case) does, however, suggest the initiation of flow leakage at very low rudder angles.

Relevant two-dimensional section data, reviewed briefly in APPENDIX A2, for aerofoils with large flaps indicates that discontinuities can occur in the lift curve even when the gap is sealed; these lift characteristics are accompanied by relatively large movements in $C\bar{P}c$. It is also evident from Ref.19 (discussed in APPENDIX A2) that a gap does allow flow leakage with consequent decrease in lift, and that increasing the gap decreased the lift slope; confirmation of this fact was reported in Ref.4.

The influence of the horizontal gap is not clear; Fig.8 includes the case of the all-movable rudder (i.e. rudder + skeg moved simultaneously) with gaps left open. It is seen that the decrease in lift curve slope relative to the gap-sealed case is small compared with the decrease for the skeg rudder $\beta = 0$ case. This would suggest that the horizontal gap is not of great significance. Further, this result also suggests that the relatively sharp decrease in growth of lift for $\beta = 0$ is due primarily to the build up of separation over the flapped portion of the rudder (behind skeg) as compared with being due to flow leakage.

Fig.8 gives an indication of the influence of Reynolds Number, Rn, for the $\beta = 0$ case; as would be expected, there is no significant change in the lift curve slope for small angles of attack. Similarly after the reduction in the lift curve slope there is very little difference in slopes. $C_{L\,max}$ and α_{STALL} are reduced slightly for the lower Rn, which follows expected trends. It is seen, however, that the reduction in lift curve slope is delayed for the lower Rn. Reduced Rn tests were also made for $\beta = 4.75^{\circ}$ and 9.75°, Figs.5e and 5f; for $\beta = 4.75^{\circ}$ there is only a slight delay in

slope change but for $\beta = 9.75^{\circ}$ the delay is similar to that for $\beta = 0$ in Fig.8.

The result for $\beta = 0$ with the transition strip removed is also shown in Fig.8. The lift curve slope is slightly larger up to about $7\frac{1}{2}^{\circ}$ but, unlike the case with transition strip, continues up until about $\alpha = 15^{\circ}$ before the slope suddenly decreases. This result is in agreement with the results presented in Ref.14 which show that the effect of leading edge roughness is to decrease the lift curve slope for wing sections having thickness ratios of 18% or more; the effect increases with increase in thickness ratio. A decrease in lift curve slope and earlier stall for aerofoils with leading edge roughness is also reported in Ref.1. Extended laminar flow is likely without the use of roughness and, with the thin turbulent boundary layer which then develops downstream, separation is likely to be delayed. Further, the reduced momentum in the laminar boundary layer in the case of the test without transition strip, or the turbulent boundary layer for the reduced Rn case, is less capable of promoting gap flow.

The results of this Report, and supporting published data with gap sealed, suggest that the overall characteristic discontinuity in the growth of the lift curve for the skeg rudder is due primarily to the semi-flapped rudder configuration, and early build up of separation behind the skeg; this would also account for the relatively large movement of $C\bar{P}c$ for the skeg rudder. The degree to which separation is influenced by gap flow is not conclusive; the results do, however, indicate a steady build up of flow leakage until complete gap flow is established. According to published data on gap effects this would account, at least in part, for a reduction in the absolute lift curve slope.

7. CONCLUSIONS AND RECOMMENDATIONS

7.1 The overall characteristics of the simulated all-movable rudder of the present work compare favourably with existing published data. Its characteristics, therefore, form a satisfactory basis with which to compare the skeg rudder.

7.2 The skeg rudder displayed a characteristic discontinuity in the growth of lift with increasing angle of attack; a relatively sharp decrease in the growth of lift occurs followed by a steady build up of lift again as angle is further increased until stall of the complete rudder takes place. The data, supported by visual studies, indicate that the discontinuity is caused by the build up of separation leading to early stall of the movable part of the rudder behind the skeg.

7.3 The rudder plus skeg combination has distinctly different lift characteristics from the equivalent all-movable rudder with the same total area and aspect ratio. Whilst the maximum lift coefficient developed by the skeg rudder is only a little lower than the all-movable rudder, its rate of increase of lift for increasing angle of attack is considerably less. Compared with a lift curve slope of 0.048/deg. for the all-movable case, the skeg rudder (at zero skeg angle, for example) has a lift curve slope of 0.038/deg. before the discontinuity followed by approximately 0.029/deg. after the discontinuity; at angles of attack of 10° and 20° the lift coefficient for the rudder plus skeg combination is approximately 30% and 38% less than the all-movable respectively.

7.4 The results for zero skeg angle show that, of the total lift produced by the rudder plus skeg combination, about 83% of the lift is contributed by the movable part of the rudder and the remainder by the skeg. In general terms, the lift produced by the movable part of the rudder was found to be relatively independent of the skeg angle; a much greater proportion of the change in total lift of rudder plus skeg combination for variation in skeg angle was due to the relatively larger change in the lift on the skeg itself.

7.5 For the same developed lift, the skeg rudder had much higher drag than the equivalent all-movable rudder. For example, at lift coefficients of 0.250, 0.400 and 0.800 the drag of the rudder plus skeg combination for zero skeg angle was about 40%, 155% and 170% greater respectively than the equivalent all-movable rudder. It is considered that this increased drag was due to the early separation of the movable part of the rudder behind the skeg.

7.6 The skeg rudder has a large movement in its centre of pressure with change in angle of attack.

Compared with a total movement in $CP\bar{c}$ over the unstalled range of about 7% for the all-movable rudder, $CP\bar{c}$ for the skeg rudder moved aft about 22%. For most of the skeg angle range tested, the $CP\bar{c}$ for the rudder alone was forward of the stock for rudder angles up to about $12\frac{1}{2}^{\circ}$, leading to negative torques. Other published data indicate that $CP\bar{c}$ is likely to be even further forward when working in a propeller slipstream; careful choice of balance area is, therefore, required for the skeg rudder type if negative torques are to be avoided.

Compared with a movement in CPs over the unstalled range of about 4% to a maximum CPs of about 47% for the all-movable rudder, CPs for the rudder plus skeg combination moved about 11% to a maximum of about 54%. This difference in maximum CPs is evidently due to the relatively larger proportion of the load carried by the outboard 'all-movable' part of the skeg rudder after the early stall of the movable part behind the skeg.

7.7 The results show there is a steady build up of flow leakage through the rudder-skeg gap until complete gap flow is established; strong gap flow would appear to begin approximately when the part of the movable rudder behind the skeg is completely stalled. The degree to which the early separation behind the skeg is influenced by gap flow is, however, not conclusive. Existing published two-dimensional section data for aerofoils with gaps sealed would suggest that the characteristic discontinuity in lift curve, and large movement of centre of pressure, obtained for the skeg rudder is due mainly to its semi-flapped configuration, and not necessarily to gap flow. Other published data on gap effects do, however, indicate that some reduction in absolute lift curve slope would be expected due to leakage through the gap.

It is considered that the results for the skeg rudder of this Report represent realistic characteristics for the free-stream condition since the chosen gap size was typical for rudders currently fitted to a number of ships.

Some further studies on gap size and shape are, however, felt to be necessary if the influence of gap on separation and rudder performance is to be fully understood.

7.8 It is concluded that the results of the free-stream tests presented in this Report contribute to a better understanding of the performance of the skeg rudder; the results do, however, highlight the need for further investigation of the skeg rudder in order to provide a complete understanding of its operation, and to predict the most effective combination of rudder, skeg and gap parameters for a particular situation.

ACKNOWLEDGEMENTS

The writer wishes to acknowledge the support and assistance given by the following:

Professor G.J. Goodrich, who supervised the project.

The Science Research Council, who financed the project.

His wife, Andrea, for typing the Report.

NOMENCLATURE

The notation of angles and coefficients is further depicted in Fig.3.

AR_G	-	Geometric aspect ratio
C	-	Chord
$\bar{c}$	-	Mean chord
C_T	-	Tip chord
C_R	-	Root chord
$CP_{\bar{c}}$	-	Centre of pressure chordwise, measured from leading edge
CPs	-	Centre of pressure spanwise, measured from root
C_D	-	Drag coefficient
C_L	-	Lift coefficient
C_{Lmax}	-	Maximum lift coefficient
C_N	-	Normal force coefficient, normal to rudder
C_Y	-	Normal force coefficient, normal to skeg or ship
Rn	-	Reynolds Number
S	-	Rudder span
t	-	Rudder section thickness
X-Axis	-	Air flow axis = longitudinal axis of tunnel
X_β -Axis	-	Skeg axis
Y-Axis	-	Axis normal to air flow
Y_β -Axis	-	Axis normal to skeg
α	-	Rudder angle relative to flow
α_{STALL}	-	Rudder stall angle relative to flow
β	-	Skeg angle relative to flow (or ship drift angle at rudder)

δ	-	Rudder angle relative to skeg, or ship
Ω	-	Sweep of quarter chord
Skeg Area Ratio	-	$\frac{\text{Skeg area (assumed to } \mathbb{C} \text{ of stock)}}{\text{Total area (movable + skeg)}}$
Balance Area Ratio	-	$\frac{\text{Movable area forward of } \mathbb{C} \text{ of stock}}{\text{Total movable area}}$
Total Movable Area	-	Total area (movable + skeg) - Skeg area (assumed to $\mathbb{C}$ of stock)

REFERENCES

1. Jones G.W. Jr. : 'Aerodynamic Characteristics of Three Low Aspect Ratio Symmetrical Wings with Rectangular Planforms at Reynolds Numbers between 0.4×10^6 and 3.0×10^6 '. N.A.C.A. R.M.L52G18, 1952.

2. Whicker L.F. and Fehlner L.F. : 'Free Stream Characteristics of a Family of Low Aspect Ratio Control Surfaces for Application to Ship Design'. D.T.M.B. Report 933, December 1958.

3. Kato H. and Motora S. : 'Studies on Rudders with a Flap, First Report - Results of Open Water Tests'. Journal of Society of Naval Architects, Japan, Vol.124, 1968.

4. Kerwin J.E., Mandel P. and Lewis S.D. : 'An Experimental Study of a Series of Flapped Rudders'. Journal of Ship Research, S.N.A.M.E., December 1972.

5. Mandel P. : 'Some Hydrodynamic Aspects of Appendage Design'. S.N.A.M.E., 1953.

6. Hagen G.R. : 'A Contribution to the Hydrodynamic Design of Rudders'. Ministry of Defence, Third Ship Control Systems Symposium, Bath, September 1972.

7. Berlekom W.B. Van : 'Effects of Propeller Loading on Rudder Efficiency'. Royal Netherlands Naval College, Proceedings of Fourth Ship Control Systems Symposium, The Hague, October 1975.

8. Schoenherr K.E. : 'A Program for the Investigation of the Rudder Torque Problem'. Marine Technology, S.N.A.M.E., 1965.

9. Davies P.A.O.L. : 'The New 7' x 5½' and 15' x 12' Low Speed Wind Tunnel at the University of Southampton'. A.A.S.U. Report No.202.

10. Molland A.F. : 'The Design, Construction and Calibration of a Five-Component Strain Gauge Wind Tunnel Dynamometer'. University of Southampton, Ship Science Report No.1/77, 1976.

11. Molland A.F. : 'A Computer Program for the Analysis of Wind Tunnel Control Surface Data'. University of Southampton, Ship Science Report No.2/77, 1977.

12. Pope A. and Harper J.J. : 'Low Speed Wind Tunnel Testing'. John Wiley & Sons Inc.

13. Shiba H. : 'Model Experiments about the Manoeuvrability and Turning of Ships'. First Symposium on Ship Manoeuvrability, D.T.M.B. Report 1461, October 1960.

14. Abbot I.H. and Von Doenhoff A.E. : 'Theory of Wing Sections'. Dover Publications, New York 1958.

15. Kwik K.H. : 'Systemmatic Wind Tunnel Tests on Ships' Rudders'. Schiffstechnic, Vol.18, 1971.

16. Ames M.B. Jr. and Sears R.I. : 'Pressure - Distribution Investigation of an N.A.C.A. 0009 Airfoil with a 30-Percent-Chord Plain Flap and Three Tabs'. T.N. No.759, 1940.

17. Street W.G. and Ames M.B. Jr. : 'Pressure - Distribution Investigation of an N.A.C.A. 0009 Airfoil with a 50-Percent-Chord Plain Flap and Three Tabs'. T.N. No.734, N.A.C.A. 1939.

18. Ames M.B. Jr. and Sears R.I. : 'Pressure - Distribution Investigation of an N.A.C.A. 0009 Airfoil with an 80-Percent-Chord Plain Flap and Three Tabs'. T.N. No.761, N.A.C.A. 1940.

19. Sears R.I. : 'Wind-Tunnel Investigation of Control Surface Characteristics. I - Effect of Gap on the Aerodynamic Characteristics of an N.A.C.A. 0009 Airfoil with a 30-Percent-Chord Plain Flap'. Report L-377, N.A.C.A., June 1941.

20. Goett H.J. and Reeder J.P. : 'Effects of Elevator Nose Shape, Gap, Balance, and Tabs on the Aerodynamic Characteristics of a Horizontal Tail Surface'. Report No.675, N.A.C.A. 1939.

APPENDIX A1

CHOICE OF MODEL RUDDER CHARACTERISTICS

The principal particulars of the rudder are shown in Fig.1 and background reasons for the choice of these characteristics are as follows:

Geometric Aspect Ratio

Since at the design stage rudder area would usually be assumed to be some proportion of ship immersed lateral area, and rudder span some function of draught (due to aft end design characteristics) the designer does not normally have freedom of choice regarding rudder aspect ratio for a particular ship type.

A survey of recent ship completions indicates the use of a range of AR_G varying from 1.0 to 2.0.

The model rudder tested has a geometric aspect ratio of 1.5; this is considered to be a satisfactory mean value for modern ship applications and for the purposes of the basic performance tests.

It is envisaged that a future extension of the model rudder series might include aspect ratios of 1.0 and 2.0.

Taper Ratio

A study of recent ship applications indicates the use of taper ratios varying from about 0.60 up to 1.0, but with no apparent scientific background accounting for the chosen value. The rudder tested has a taper ratio of 0.59; future tests on rudders with taper ratios of 0.80 and 1.0 are projected.

Skeg Depth

The survey of recent ship applications indicates the skeg depth for the majority of the ships to be between 48% and 52% of the span. Isolated cases exist where values as low as 40% and as high as 55% have been used. Since the centre of pressure acts between 45 and 50% of the span (measured from root), and structural design analysis can be simplified by

assuming the whole rudder load to act at the lower pintle, then from the structural point of view the use of a skeg depth/rudder span ratio of between 0.45 and 0.50 would appear justified.

If outboard tailshaft removal is required in single screw/single rudder or twin screw/twin rudder designs, then existing design arrangements would indicate a maximum allowable skeg depth of about 50-55% of span. For simplicity of design, and comparative purposes, the rudder tested had a skeg depth/rudder span of 0.50 (0.496). An extension to the basic tests might entail varying the skeg depth above and below 50% for one of the rudders, whilst keeping taper ratio constant.

Skeg Area, Balance Area and Sweep of Quarter Chord

Since for a fixed skeg depth the skeg area is related to structural requirements, i.e. fore and aft length and thickness (to be discussed later), and the balance considered is the static geometric case, the chosen skeg and balance areas have been closely related to existing rudders.

A survey of published designs indicates the balance ratio for skeg rudders acting behind a propeller to be generally between 19% and 21%; a value of 19% was chosen for the basic rudder. The skeg area ratio tends to vary between 19% and 23% and a value of 20.5% was chosen for the basic rudder. In order to achieve these values for the taper ratio of 0.59, a sweep of quarter chord of 3.8^{o} is necessary.

Thickness and Section Shape of Rudders

Since thickness is related to structural requirements of rudder and skeg, a survey of existing ship rudders was made; this shows the thickness/chord ratio to vary from about 0.18 to about 0.24.

Based on this data, and the future need to compare the results with other published work, a constant thickness/chord ratio of 0.20 was used. The section chosen is the NACA 00 series; its general section characteristics are well known and are suitable for the proposed application; a further desirable feature is that its maximum thickness is 30% aft of leading edge which is close to the likely position of the rudder stock and pintles.

Radial and Horizontal Gaps between Movable Rudder and Skeg

The gaps for eight rudders for fast cargo and container ships were analysed. These tended to vary between 25mm and 50mm, and were independent of absolute rudder size; such gaps will, of course, cover the provisions for adequate access for cleaning and maintenance. The analysis indicated the gap/mean chord ratio to vary between about 0.005 and about 0.014.

A compromise gap size of 4mm was chosen for the model rudder, resulting in a gap/chord ratio of 0.009.

Although other experimenters (e.g. Refs. 4 and 15) have used smaller values, the chosen gap ratio is considered to represent a realistic ship value.

APPENDIX A2

BRIEF REVIEW OF SOME TWO-DIMENSIONAL SECTION DATA FOR FLAPPED AEROFOILS

In an attempt to provide a better understanding of the performance characteristics (in particular, lift) of the rudder described in the present work, a brief review was made of some early published work on flapped aerofoils, Refs.16, 17, 18, 19. This was felt necessary since, for example, neither the results in Ref.6, for semi-balanced rudders, nor cross-plots of the data for flapped rudders in Ref.4, indicate discontinuities in the growth of the lift curve.

Specific results, and cross-plottings, from Refs.16, 17, 18, 19 are presented in Fig.11 (for clarity, the Nomenclature of the present Report is used). Considering first the data for variation in angle of attack with gap sealed, Fig.11(a), the results indicate clearly a relatively sharp decrease in the growth of the lift curve as separation builds up and stall occurs on the flapped part of the aerofoil, followed by a steady increase in lift with further increase in angle of attack. This effect is more pronounced as the ratio of flap (or rudder) size is increased as a proportion of the total rudder plus skeg combination. The most extreme case tended to be for $\beta = -4\frac{1}{2}^{\circ}$ (Fig.11(b)) for which a very pronounced discontinuity occurs; Fig.11(b) also includes the lift produced by the skeg alone for which a similar discontinuity occurs. The variation in $CP\bar{c}$ with angle, also included in Fig.11(a), for the flapped foils is seen to be large; as would be expected, the movement in $CP\bar{c}$ decreases with increasing flap size.

Ref.19 investigated the influence of gap size on performance for a 30% flap and cross-plots of the results are shown in Fig.11(c); it is seen that the lift curve slope decreases as gap size is increased. The trend of the curves does, however, suggest that whilst there is a distinct loss in lift due to gap (e.g. about 20% for the $0.010\bar{c}$ gap at 20°) the difference in effect between, say, the $0.005\bar{c}$ gap and $0.010\bar{c}$ gap is not large. This conclusion was also arrived at in Ref.20. Further, the influence of a gap appears to diminish at larger angles of attack; this effect

is also reported in Ref.4.

A general conclusion drawn from this brief review is that whilst the presence of a gap influences the lift curve slope, its presence is not of necessity in order to produce a discontinuity in the lift curve of a flapped lifting surface.

APPENDIX A3

TABULATED TEST RESULTS

REYNOLDS NO. = 1.23000E+06

SKEG ANGLE, BETA(DEG.) = -15.25

	AA	AD	CL	CN	CY	CD	CPC	CPS
(A)	-20.92	-5.67	-.872	-.896	-.9	.229	28.24	47.84
(A)	-18.35	-3.1	-.78	-.799	-.8	.185	26.61	46.98
(B)	-18.35	-3.1	-.449	-.472	-.469	.145	38.06	63.37
(C)	-18.35	-3.1	-.331			.04	10.4	23.48
(A)	-15.82	-.57	-.737	-.747	-.746	.14	23.41	44.52
(B)	-15.82	-.57	-.394	-.405	-.403	.096	33.76	66.63
(C)	-15.82	-.57	-.343			.044	11.25	18.52
(A)	-13.24	2.01	-.632	-.638	-.634	.099	20.79	46.01
(B)	-13.24	2.01	-.34	-.346	-.344	.066	30.78	65.48
(C)	-13.24	2.01	-.292			.033	8.83	23.01
(A)	-10.64	4.61	-.509	-.513	-.508	.069	17.24	46.19
(B)	-10.64	4.61	-.263	-.265	-.262	.037	26.86	64.35
(C)	-10.64	4.61	-.246			.032	6.74	26.97
(A)	-8.06	7.19	-.401	-.404	-.4	.051	13.89	45.39
(B)	-8.06	7.19	-.174	-.175	-.172	.016	21.47	73.63
(C)	-8.06	7.19	-.227			.035	7.95	23.95
(A)	-5.4	9.85	-.199	-.201	-.2	.032	3.84	42.37
(B)	-5.4	9.85	-.102	-.103	-.099	.002	10.55	84.18
(C)	-5.4	9.85	-.097			.03	-2.24	97
(A)	-.33	14.92	-.106	-.106	-.111	.033	-14.43	36.39
(B)	-.33	14.92	.044	.044	.042	.003	54.59	-8.28
(C)	-.33	14.92	-.15			.03	6.36	23.38

AA=RUDDER ANGLE,ALPHA(DEG.), AD=RUDDER ANGLE,DELTA(DEG.)
CL=LIFT COEFFICIENT, CN=RUDDER NORMAL COEFFICIENT
CY=SHIP NORMAL COEFFIENT, CD=DRAG COEFFICIENT
CPC=C OF P CHORD(%C), CPS=C OF P SPAN(%S)
ALL COEFFICIENTS BASED ON TOTAL AREA OF RUDDER PLUS SKEG

(A)=RUDDER PLUS SKEG, (B)=RUDDER ALONE, (C)=SKEG ALONE

Continued

(A)	2.24	17.49	-.009	-.008	-.017	.033	-524.1	50.72
(B)	2.24	17.49	.118	.119	.11	.016	43.3	54.46
(C)	2.24	17.49	-.127			.017	9.29	27.91
(A)	4.82	20.07	.089	.093	.074	.046	30.53	55.57
(B)	4.82	20.07	.193	.2	.183	.031	42.65	39.77
(C)	4.82	20.07	-.109			.015	10.51	17.45
(A)	7.35	22.6	.127	.134	.105	.066	70.89	60.14
(B)	7.35	22.6	.264	.267	.245	.039	42.25	38.72
(C)	7.35	22.6	-.137			.027	14.28	17.69
(A)	9.87	25.12	.155	.168	.127	.087	62.77	63.31
(B)	9.87	25.12	.269	.276	.244	.062	38.79	51.93
(C)	9.87	25.12	-.114			.025	4.1	31.26
(A)	12.41	27.66	.205	.223	.17	.106	52.96	64.12
(B)	12.41	27.66	.304	.315	.272	.082	38.39	50.59
(C)	12.41	27.66	-.099			.024	6.15	16.34
(A)	14.97	30.22	.29	.31	.25	.115	46.99	58.02
(B)	14.97	30.22	.341	.356	.302	.103	38.53	54.75
(C)	14.97	30.22	-.051			.012	-11.6	34.22
(A)	17.52	32.77	.346	.372	.297	.14	44.11	60.44
(B)	17.52	32.77	.394	.412	.349	.122	38.46	55.41
(C)	17.52	32.77	-.048			.018	-2.61	12.25
(A)	20.09	35.34	.44	.469	.382	.163	41.92	56.09
(B)	20.09	35.34	.452	.474	.399	.145	39.06	54.79
(C)	20.09	35.34	-.012			.018	-45.88	-9.74
(A)	22.83	38.08	.491	.529	.422	.198	41.3	58.6
(B)	22.83	38.08	.508	.535	.446	.172	39.01	56.71
(C)	22.83	38.08	-.017			.026	-14.35	41.83
(A)	25.79	41.04	.574	.62	.492	.238	40.67	58.94
(B)	25.79	41.04	.571	.603	.498	.205	39.31	57.62
(C)	25.79	41.04	.003			.033	-106.7	40.39

TABULATED TEST RESULTS

REYNOLDS NO. = 1.23000E+06

SKEG ANGLE, BETA(DEG.) = -10.25

	AA	AD	CL	CN	CY	CD	CPC	CPS
(A)	-15.78	-5.53	-.688	-.699	-.7	.135	26.16	45.65
(B)	-15.78	-5.53	-.409	-.423	-.421	.109	35.47	61.38
(C)	-15.78	-5.53	-.279			.026	12.2	21.68
(A)	-13.23	-2.98	-.622	-.629	-.629	.103	24.04	44.11
(B)	-13.23	-2.98	-.362	-.369	-.368	.071	32.74	63.31
(C)	-13.23	-2.98	-.26			.032	11.8	21.19
(A)	-10.64	-.39	-.507	-.512	-.512	.075	20.56	44.88
(B)	-10.64	-.39	-.271	-.274	-.274	.044	29.26	63.84
(C)	-10.64	-.39	-.236			.031	10.52	22.98
(A)	-8.05	2.2	-.385	-.388	-.387	.048	17.44	44.7
(B)	-8.05	2.2	-.195	-.197	-.196	.025	25.62	64.91
(C)	-8.05	2.2	-.19			.023	8.97	23.96
(A)	-5.46	4.79	-.278	-.28	-.28	.037	13.97	42.97
(B)	-5.46	4.79	-.114	-.114	-.114	.008	19.63	73
(C)	-5.46	4.79	-.164			.029	10.13	22.25
(A)	-2.89	7.36	-.186	-.187	-.188	.029	9.76	39.79
(B)	-2.89	7.36	-.043	-.043	-.042	-.002	8.51	191.46
(C)	-2.89	7.36	-.143			.031	10.46	21.87
(A)	-.31	9.94	-.032	-.032	-.036	.026	-8	36.53
(B)	-.31	9.94	.028	.028	.028	-.002	54.01	-13.41
(C)	-.31	9.94	-.11			.028	8.4	22.71
(A)	2.26	12.51	.011	.012	.006	.027	249.74	158.99
(B)	2.26	12.51	.098	.098	.095	.009	36.33	36.09
(C)	2.26	12.51	-.087			.018	8.04	19.11
(A)	4.84	15.09	.113	.115	.106	.03	51.93	53.56
(B)	4.84	15.09	.176	.177	.17	.02	38.71	44.21
(C)	4.84	15.09	-.063			.01	15.11	27.24
(A)	7.36	17.61	.142	.149	.109	.06	54.58	65.09
(B)	7.36	17.61	.236	.239	.226	.037	37.99	43.73
(C)	7.36	17.61	-.094			.023	10.52	19.75

AA=RUDDER ANGLE, ALPHA(DEG.), AD=RUDDER ANGLE, DELTA(DEG.)
CL=LIFT COEFFICIENT, CN=RUDDER NORMAL COEFFICIENT
CY=SHIP NORMAL COEFFIENT, CD=DRAG COEFFICIENT
CPC=C OF P CHORD(%C), CPS=C OF P SPAN(%S)
ALL COEFFICIENTS BASED ON TOTAL AREA OF RUDDER PLUS SKEG
(A)=RUDDER PLUS SKEG, (B)=RUDDER ALONE, (C)=SKEG ALONE

Continued

(A)	9.89	20.14	.182	.193	.165	.078	48.73	63.79
(B)	9.89	20.14	.297	.303	.282	.058	38.36	46.85
(C)	9.89	20.14	-.115			.02	21.1	15.71
(A)	12.44	22.69	.252	.265	.238	.069	43.22	54.23
(B)	12.44	22.69	.293	.303	.274	.073	36.72	56.75
(C)	12.44	22.69	-.041			.011	-4.12	68.81
(A)	14.99	25.24	.306	.324	.282	.11	40.26	60.17
(B)	14.99	25.24	.353	.366	.33	.097	37.11	54.43
(C)	14.99	25.24	-.047			.013	15.95	9.18
(A)	17.56	27.81	.401	.422	.372	.13	38.91	55.84
(B)	17.56	27.81	.392	.41	.365	.119	37.71	57.45
(C)	17.56	27.81	.009			.011	109.64	2.74
(A)	20.1	30.35	.458	.483	.423	.155	38.18	58.61
(B)	20.1	30.35	.458	.471	.408	.143	38.67	56.22
(C)	20.1	30.35	.006	.012	.005	.012	.56	335.37
(A)	22.67	32.92	.545	.574	.504	.184	37.66	55.57
(B)	22.67	32.92	.499	.525	.462	.163	38.57	59.36
(C)	22.67	32.92	.046			.016	26.58	20.87
(A)	25.22	35.47	.608	.643	.561	.218	37.36	55.69
(B)	25.22	35.47	.568	.598	.524	.198	39.13	57.3
(C)	25.22	35.47	.04			.02	8.49	39.1
(A)	27.98	38.23	.687	.726	.632	.255	38.17	54.53
(B)	27.98	38.23	.615	.651	.565	.229	39.48	59.79
(C)	27.98	38.23	.072			.026	25.8	9.81
(A)	30.96	41.21	.785	.827	.72	.299	38.5	53.31
(B)	30.96	41.21	.679	.723	.621	.274	40.49	59.2
(C)	30.96	41.21	.106			.025	24.3	10.51

TABULATED TEST RESULTS

REYNOLDS NO. = 1.23000E+06

SKEG ANGLE, BETA(DEG.) = -5.25

	AA	AD	CL	CN	CY	CD	CPC	CPS
(A)	-10.61	-5.36	-.471	-.477	-.476	.074	24.94	46.79
(B)	-10.61	-5.36	-.298	-.302	-.301	.048	33.11	58.4
(C)	-10.61	-5.36	-.173			.026	10.8	26.87
(A)	-8.03	-2.78	-.362	-.365	-.365	.05	21.6	45.32
(B)	-8.03	-2.78	-.211	-.213	-.213	.028	28.45	61.42
(C)	-8.03	-2.78	-.151			.022	11.98	22.3
(A)	-5.44	-.19	-.249	-.251	-.251	.035	18.22	45.01
(B)	-5.44	-.19	-.131	-.131	-.131	.011	24.32	64.29
(C)	-5.44	-.19	-.118			.024	11.58	24
(A)	-2.87	2.38	-.156	-.157	-.158	.028	15.24	42.31
(B)	-2.87	2.38	-.056	-.056	-.055	-.001	19.02	76.64
(C)	-2.87	2.38	-.1			.029	13.38	23.57
(A)	-.29	4.96	-.054	-.054	-.056	.023	.86	38.99
(B)	-.29	4.96	.01	.01	.01	-.004	52.98	-53.55
(C)	-.29	4.96	-.064			.027	9.98	24.32
(A)	2.28	7.53	.043	.044	.041	.023	48.03	55.52
(B)	2.28	7.53	.074	.074	.073	-.001	28.39	41.96
(C)	2.28	7.53	-.031			.024	3.52	22.32
(A)	4.85	10.1	.13	.132	.127	.03	33.72	52.47
(B)	4.85	10.1	.149	.15	.147	.014	31.02	48.74
(C)	4.85	10.1	-.019			.016	13.67	19.59
(A)	7.43	12.68	.227	.231	.222	.042	34.7	50.83
(B)	7.43	12.68	.235	.238	.231	.035	36.89	47.85
(C)	7.43	12.68	-.008			.007	96.3	-61.17
(A)	9.95	15.2	.254	.262	.247	.066	36.71	57.1
(B)	9.95	15.2	.293	.298	.287	.055	36.39	53.91
(C)	9.95	15.2	-.039			.011	34.29	41.29

AA=RUDDER ANGLE, ALPHA(DEG.), AD=RUDDER ANGLE, DELTA(DEG.)
CL=LIFT COEFFICIENT, CN=RUDDER NORMAL COEFFICIENT
CY=SHIP NORMAL COEFFIENT, CD=DRAG COEFFICIENT
CPC=C OF P CHORD(%C), CPS=C OF P SPAN(%S)
ALL COEFFICIENTS BASED ON TOTAL AREA OF RUDDER PLUS SKEG

(A)=RUDDER PLUS SKEG, (B)=RUDDER ALONE, (C)=SKEG ALONE

Continued

(A)	12.49	17.74	.305	.317	.296	.037	35.7	56.76
(B)	12.49	17.74	.33	.337	.322	.069	36.03	54.88
(C)	12.49	17.74	-.025			.018	39.9	17.24
(A)	15.02	20.27	.35	.366	.339	.106	34.45	58.13
(B)	15.02	20.27	.359	.37	.349	.09	35.55	51.15
(C)	15.02	20.27	-.009			.016	74.51	-236.71
(A)	17.59	22.84	.435	.452	.422	.123	34.3	56.35
(B)	17.59	22.84	.398	.415	.386	.117	36.72	57.44
(C)	17.59	22.84	.037			.006	6.07	46.79
(A)	20.15	25.4	.521	.541	.506	.15	34.3	53.2
(B)	20.15	25.4	.462	.482	.448	.14	37.22	55.47
(C)	20.15	25.4	.059			.01	9.97	37.21
(A)	22.7	27.95	.585	.607	.567	.175	34.46	54.6
(B)	22.7	27.95	.52	.545	.503	.169	37.63	57.49
(C)	22.7	27.95	.065			.006	7.71	29.57
(A)	25.26	30.51	.659	.686	.638	.211	34.85	54.07
(B)	25.26	30.51	.566	.595	.547	.194	38.4	58.94
(C)	25.26	30.51	.093			.017	11.75	23.28
(A)	27.8	33.05	.719	.752	.694	.249	35.86	54.64
(B)	27.8	33.05	.621	.659	.597	.236	39.07	59.76
(C)	27.8	33.05	.098			.013	14.07	19.56
(A)	30.36	35.61	.797	.838	.767	.297	36.63	54.11
(B)	30.36	35.61	.681	.723	.654	.263	40.1	59.75
(C)	30.36	35.61	.116			.029	14.56	18.3
(A)	33.09	38.34	.834	.891	.799	.352	38.43	53.86
(B)	33.09	38.34	.717	.772	.686	.314	41.53	59.23
(C)	33.09	38.34	.117			.038	17.4	16.93
(A)	36.01	41.26	.853	.926	.813	.402	38.77	52.13
(B)	36.01	41.26	.687	.767	.652	.36	43.04	61.15
(C)	36.01	41.26	.166			.042	18.51	9.99

APPENDIX A3 (Continued)

TABULATED TEST RESULTS

REYNOLDS NO. = 1.23000E+06

SKEG ANGLE, BETA(DEG.) = -.25

	AA	AD	CL	CN	CY	CD	CPC	CPS
(A)	-5.41	-5.16	-.213	-.215	-.214	.035	23.84	46.47
(B)	-5.41	-5.16	-.149	-.15	-.149	.014	28.08	55.57
(C)	-5.41	-5.16	-.064			.021	13.7	25.39
(A)	-2.85	-2.6	-.134	-.135	-.134	.026	24.78	44.55
(B)	-2.85	-2.6	-.074	-.074	-.074	.002	26.15	59.25
(C)	-2.85	-2.6	-.06			.024	22.91	26.48
(A)	-.27	-.02	-.031	-.031	-.031	.022	31.04	40.46
(B)	-.27	-.02	-.007	-.007	-.007	-.005	35.69	91.09
(C)	-.27	-.02	-.024			.027	29.72	25.87
(A)	2.3	2.55	.07	.071	.07	.023	18.03	43.62
(B)	2.3	2.55	.059	.059	.059	-.004	22.43	56.4
(C)	2.3	2.55	.011			.027	-8.78	-26.99
(A)	4.88	5.13	.163	.17	.168	.025	21.74	47.55
(B)	4.88	5.13	.127	.127	.127	.006	25.39	56.82
(C)	4.88	5.13	.041			.019	10.07	22.19
(A)	7.45	7.7	.265	.267	.265	.036	25.39	46.81
(B)	7.45	7.7	.211	.212	.211	.022	29.47	58.64
(C)	7.45	7.7	.054			.014	9.11	24.9
(A)	10	10.25	.328	.333	.328	.056	28.59	46.06
(B)	10	10.25	.294	.298	.294	.047	32.49	51.65
(C)	10	10.25	.034			.009	-6.26	24.84

AA=RUDDER ANGLE, ALPHA(DEG.), AD=RUDDER ANGLE, DELTA(DEG.)
CL=LIFT COEFFICIENT, CN=RUDDER NORMAL COEFFICIENT
CY=SHIP NORMAL COEFFIENT, CD=DRAG COEFFICIENT
CPC=C OF P CHORD(%C), CPS=C OF P SPAN(%S)
ALL COEFFICIENTS BASED ON TOTAL AREA OF RUDDER PLUS SKEG

(A)=RUDDER PLUS SKEG, (B)=RUDDER ALONE, (C)=SKEG ALONE

Continued

(A)	12.54	12.79	.379	.387	.379	.079	29.51	50.42
(B)	12.54	12.79	.361	.369	.36	.076	35.23	56.1
(C)	12.54	12.79	.018			.003	-83.34	-59.8
(A)	15.08	15.33	.43	.44	.429	.094	29.84	53.56
(B)	15.08	15.33	.375	.385	.374	.087	34.3	57.09
(C)	15.08	15.33	.055			.007	-1.24	24
(A)	17.63	17.88	.494	.506	.493	.117	30.41	54.22
(B)	17.63	17.88	.42	.435	.419	.116	35.32	57.46
(C)	17.63	17.88	.074			.001	1.81	34.33
(A)	20.19	20.44	.576	.59	.575	.143	31.22	53.04
(B)	20.19	20.44	.47	.489	.469	.139	35.77	58.91
(C)	20.19	20.44	.106			.004	10.43	25.5
(A)	22.74	22.99	.633	.65	.633	.172	31.75	53.53
(B)	22.74	22.99	.539	.562	.539	.169	37.63	57.33
(C)	22.74	22.99	.094			.003	-3.2	30.94
(A)	25.29	25.54	.706	.729	.705	.213	32.99	52.31
(B)	25.29	25.54	.582	.613	.581	.204	38.73	59.54
(C)	25.29	25.54	.124			.009	4.94	16.55
(A)	27.84	28.09	.762	.789	.761	.247	34.33	54.49
(B)	27.84	28.09	.64	.676	.639	.235	39.54	59.14
(C)	27.84	28.09	.122			.012	5.54	27.47
(A)	30.38	30.63	.813	.856	.811	.306	36.1	53.45
(B)	30.38	30.63	.667	.714	.666	.274	41.26	59.53
(C)	30.38	30.63	.146			.032	10.84	25.32
(A)	32.92	33.17	.866	.916	.864	.348	37	52.66
(B)	32.92	33.17	.697	.757	.696	.317	42.14	60.29
(C)	32.92	33.17	.169			.031	13.9	19.12
(A)	35.41	35.66	.856	.928	.854	.397	37.54	53.92
(B)	35.41	35.66	.662	.743	.661	.351	43.54	62.29
(C)	35.41	35.66	.194			.046	14.54	22.43
(A)	37.94	38.19	.639	.764	.637	.423	40.91	46.24
(B)	37.94	38.19	.491	.618	.489	.376	47.59	50.72
(C)	37.94	38.19	.148			.047	11.75	22.76

REYNOLDS NO. = 1.23000E+06

SKEG ANGLE, BETA(DEG.) = 4.75

	AA	AD	CL	CN	CY	CD	CPC	CPS
(A)	-5.4	-10.15	-.196	-.198	-.192	.034	33.98	46.58
(A)	-2.82	-7.57	-.09	-.091	-.086	.024	40.94	47.07
(A)	-.24	-4.99	.009	.009	.01	.019	-154.18	21.93
(B)	-.24	-4.99	-.023	-.023	-.023	-.003	43.79	23.44
(C)	-.24	-4.99	.032			.022	-9.09	23.18
(A)	2.32	-2.43	.097	.098	.099	.018	3.94	43.76
(B)	2.32	-2.43	.039	.039	.038	-.005	9.07	76.94
(C)	2.32	-2.43	.058			.023	1.12	22.32
(A)	4.9	.15	.194	.196	.195	.026	13.75	46.66
(B)	4.9	.15	.113	.113	.113	.003	21.82	63.76
(C)	4.9	.15	.081			.023	2.82	23.47
(A)	7.48	2.73	.299	.301	.301	.035	18.78	46.24
(B)	7.48	2.73	.183	.183	.184	.015	26.56	60.96
(C)	7.48	2.73	.116			.02	6.52	23.28
(A)	10.06	5.31	.401	.404	.404	.05	22.95	47.45
(B)	10.06	5.31	.272	.274	.274	.036	31.22	59.13
(C)	10.06	5.31	.122			.014	5.43	22.8
(A)	12.6	7.85	.504	.507	.504	.073	25.75	49.4
(B)	12.6	7.85	.342	.344	.341	.06	33.67	59.43
(C)	12.6	7.85	.113			.013	1.3	19.09
(A)	15.15	10.4	.513	.521	.519	.097	26.85	48.81
(B)	15.15	10.4	.39	.399	.396	.085	34.72	60.45
(C)	15.15	10.4	.123			.012	1.56	10.66
(A)	17.69	12.94	.573	.582	.58	.12	27.28	51.07
(B)	17.69	12.94	.448	.46	.455	.108	34.53	57.14
(C)	17.69	12.94	.125			.012	.97	28.53
(A)	20.24	15.49	.635	.645	.644	.142	28.25	50.68
(B)	20.24	15.49	.461	.48	.47	.136	35.64	62.64
(C)	20.24	15.49	.174			.006	8.2	16.33
(A)	22.79	18.04	.699	.711	.71	.173	29.07	51.54
(B)	22.79	18.04	.54	.562	.552	.165	37.18	57.62
(C)	22.79	18.04	.159			.008	.82	29.67
(A)	25.32	20.57	.739	.759	.754	.213	31.03	53.17
(A)	27.86	23.11	.797	.827	.815	.262	33.25	52.6
(A)	30.42	25.67	.868	.905	.89	.309	34.33	51.9
(A)	32.97	28.22	.929	.975	.954	.359	35.44	51.06
(A)	35.47	30.72	.929	.989	.958	.4	35.94	50.03
(A)	37.79	33.04	.697	.812	.73	.426	38.59	44.47

* AA=RUDDER ANGLE, ALPHA(DEG.), AD=RUDDER ANGLE, DELTA(DEG.)
CL=LIFT COEFFICIENT, CN=RUDDER NORMAL COEFFICIENT
CY=SHIP NORMAL COEFFIENT, CD=DRAG COEFFICIENT
CPC=C OF P CHORD(%C), CPS=C OF P SPAN(%S)
ALL COEFFICIENTS BASED ON TOTAL AREA OF RUDDER PLUS SKEG

(A)=RUDDER PLUS SKEG, (B)=RUDDER ALONE, (C)=SKEG ALONE

REYNOLDS NO. = 1.23000E+06

SKEG ANGLE, BETA(DEG.) = 9.75

	AA	AD	CL	CN	CY	CD	CPC	CPS
(A)	-5.38	-15.13	-.171	-.174	-.162	.041	46.36	50.28
(A)	-2.79	-12.54	-.058	-.059	-.052	.027	76.72	61.21
(A)	-.22	-9.97	.037	.037	.04	.021	-57.68	29.1
(B)	-.22	-9.97	-.045	-.045	-.044	0	48.37	11.55
(C)	-.22	-9.97	.082			.021	1.59	20.23
(A)	2.35	-7.4	.124	.125	.125	.019	-2.89	43.92
(A)	4.92	-4.83	.224	.225	.225	.024	8.95	44.7
(B)	4.92	-4.83	.089	.089	.087	-.001	13.27	76.97
(C)	4.92	-4.83	.135			.025	6.29	24.12
(A)	7.49	-2.26	.316	.318	.317	.033	14.16	46.98
(A)	10.06	.31	.4	.401	.4	.04	16.79	52.05
(B)	10.06	.31	.241	.242	.242	.027	27.85	63.31
(C)	10.06	.31	.159			.013	-.05	34.92
(A)	12.65	2.9	.516	.518	.52	.068	21.66	48.22
(A)	15.21	5.46	.597	.6	.603	.092	24.54	47.86
(B)	15.21	5.46	.36	.369	.368	.081	34.49	63.52
(C)	15.21	5.46	.237			.011	9.12	22.96
(A)	17.73	7.98	.622	.628	.632	.117	25.3	49.71
(A)	20.29	10.54	.706	.71	.719	.139	26.07	50.15
(B)	20.29	10.54	.492	.511	.509	.142	37.23	58.42
(C)	20.29	10.54	.214			-.003	-.56	28.79
(A)	22.84	13.09	.771	.779	.789	.176	27.72	49.27
(A)	25.37	15.62	.801	.823	.828	.231	31.58	50.58
(A)	27.91	18.16	.857	.886	.89	.275	32.5	51.25
(A)	30.45	20.7	.912	.942	.949	.308	33.45	51.95
(A)	33	23.25	.971	1.017	1.019	.372	34.18	51.57
(A)	35.53	25.78	1.008	1.059	1.061	.41	34.67	51.17
(A)	38.06	28.31	1.046	1.109	1.107	.463	35.73	51.13
(A)	30.34	30.59	.761	.887	.829	.474	37.91	44.12
(A)	42.34	32.59	.76	.904	.834	.568	38.48	44.95

REYNOLDS NO. = 1.23000E+06

SKEG ANGLE, BETA(DEG.) = 14.75

	AA	AD	CL	CN	CY	CD	CPC	CPS
(A)	-.2	-14.95	.064	.064	.068	.026	-46.19	30.43
(A)	10.1	-4.65	.454	.456	.452	.051	15.8	44.75
(A)	15.25	.5	.648	.649	.649	.09	21.58	46.85
(A)	20.32	5.57	.74	.754	.758	.172	27.67	51.31

APPENDIX A3 (Continued)

TABULATED TEST RESULTS

REYNOLDS NO. = 860000

SKEG ANGLE,BETA(DEG.) = -.25

	AA	AD	CL	CN	CY	CD	CPC	CPS
(A)	-.27	-.02	-.025	-.025	-.025	.022	36.67	42.86
(B)	-.27	-.02	-.007	-.007	-.004	.004	36.96	118.36
(C)	-.27	-.02	-.018			.026	36.55	10.48
(A)	4.85	5.13	.165	.166	.165	.024	21.18	48.85
(B)	4.83	5.13	.132	.132	.131	.005	25.57	54.38
(C)	4.88	5.13	.033			.019	3.52	27.99
(A)	10.03	10.28	.361	.365	.36	.052	28.38	48.88
(B)	10.03	10.28	.305	.309	.305	.047	33.6	52.26
(C)	10.03	10.28	.056			.005	-.77	29.16
(A)	12.55	12.8	.391	.398	.391	.077	29.93	55.15
(A)	15.09	15.34	.443	.453	.443	.096	29.78	53.07
(B)	15.09	15.34	.372	.383	.372	.09	34.68	58.79
(C)	15.09	15.34	.071			.006	3.25	19.94
(A)	20.2	20.45	.581	.596	.58	.147	31.26	54.78
(B)	20.2	20.45	.461	.481	.46	.141	36.78	60.73
(C)	20.2	20.45	.12			.006	9.43	29.49
(A)	25.31	25.57	.734	.753	.733	.21	32.49	52.55
(B)	25.31	25.57	.577	.607	.576	.199	38.67	59.19
(C)	25.31	25.57	.157			.011	8.86	25.9
(A)	27.85	28.1	.773	.804	.772	.258	34.2	54.38
(B)	27.85	28.1	.635	.673	.634	.239	40.06	58.18
(C)	27.85	28.1	.138			.019	5.77	38.93
(A)	30.39	30.64	.832	.863	.831	.288	35.23	53.12
(B)	30.39	30.64	.66	.709	.659	.277	41.03	60.49
(C)	30.39	30.64	.172			.011	11.46	20.14
(A)	32.9	33.15	.842	.893	.841	.342	37	54.93
(B)	32.9	33.15	.682	.743	.681	.313	42.54	60.34
(C)	32.9	33.15	.16			.029	11.33	30.78
(A)	35.26	35.51	.662	.762	.66	.383	39.29	45.01
(B)	35.26	35.51	.467	.582	.466	.348	47.24	52.96
(C)	35.26	35.51	.195			.035	15.47	18.21

REYNOLDS NO. = 860000

SKEG ANGLE,BETA(DEG.) = 4.75

	AA	AD	CL	CN	CY	CD	CPC	CPS
(A)	-.24	-4.99	.007	.007	.009	.022	-226.01	56.06
(B)	-.24	-4.99	-.021	-.021	-.021	-.001	43.36	22.52
(C)	-.24	-4.99	.028			.023	-17.85	30.4
(A)	4.9	.15	.198	.2	.2	.027	14.48	46.09
(B)	4.9	.15	.116	.116	.116	.003	22.7	63.2
(C)	4.9	.15	.082			.024	3.12	22.42
(A)	10.06	5.31	.402	.405	.405	.051	22.54	48.03
(B)	10.06	5.31	.274	.277	.277	.042	31.25	58.91
(C)	10.06	5.31	.128			.009	3.81	24.46
(A)	15.15	10.4	.513	.52	.519	.096	27.27	51.49
(B)	15.15	10.4	.41	.42	.416	.091	36.68	59.35
(C)	15.15	10.4	.103			.005	-10.6	19.03
(A)	20.24	15.49	.637	.648	.647	.145	28.58	51.91
(B)	20.24	15.49	.479	.495	.488	.132	36.58	60.7
(C)	20.24	15.49	.158			.013	4.01	24.43
(A)	22.8	18.05	.707	.72	.718	.176	29.38	52.44
(B)	22.8	18.05	.561	.581	.572	.166	37.58	56.19
(C)	22.8	18.05	.146			.01	-2.82	37.72
(A)	25.33	20.58	.754	.774	.769	.217	31.37	51.12
(B)	25.33	20.58	.646	.678	.661	.219	40.36	55.78
(C)	25.33	20.58	.108			-.002	-24.38	22.37
(A)	30.42	25.67	.863	.901	.885	.31	34.16	52.67
(B)	30.42	25.67	.698	.746	.718	.284	43.62	57.72
(C)	30.42	25.67	.165			.026	-7.81	31.68
(A)	32.94	28.19	.9	.941	.924	.342	35.51	54.41
(B)	32.94	28.19	.737	.803	.762	.339	42.8	57.61
(C)	32.94	28.19	.163			.003	-.37	29.62
(A)	35.25	30.5	.654	.761	.684	.393	38.22	45.52
(B)	35.25	30.5	.463	.587	.491	.362	49.52	54.78
(C)	35.25	30.5	.191			.031	3.7	14.21

AA=RUDDER ANGLE,ALPHA(DEG.), AD=RUDDER ANGLE,DELTA(DEG.)
CL=LIFT COEFFICIENT, CN=RUDDER NORMAL COEFFICIENT
CY=SHIP NORMAL COEFFIENT, CD=DRAG COEFFICIENT
CPC=C OF P CHORD(%C), CPS=C OF P SPAN(%S)
ALL COEFFICIENTS BASED ON TOTAL AREA OF RUDDER PLUS SKEG
(A)=RUDDER PLUS SKEG, (B)=RUDDER ALONE, (C)=SKEG ALONE

TABULATED TEST RESULTS

REYNOLDS NO. = 860000

SKEG ANGLE, BETA(DEG.) = 9.75

	AA	AD	CL	CN	CY	CD	CPC	CPS
(A)	-.22	-9.97	.041	.041	.044	.023	-49.26	37.06
(B)	-.22	-9.97	-.044	-.044	-.045	-.006	51.24	-56.03
(C)	-.22	-9.97	.085			.029	4.38	-10.5
(A)	4.93	-4.82	.228	.229	.229	.026	9.46	43.99
(B)	4.93	-4.82	.097	.096	.095	-.005	15.27	74.64
(C)	4.93	-4.82	.131			.031	5.51	21.67
(A)	10.06	.33	.428	.429	.429	.043	17.98	47.68
(B)	10.08	.33	.258	.258	.259	.025	26.39	61.38
(C)	10.08	.33	.17			.018	5.26	25.43
(A)	15.22	5.47	.615	.618	.621	.093	24.62	47.37
(B)	15.22	5.47	.42	.424	.425	.073	34.03	54.91
(C)	15.22	5.47	.195			.02	4.39	30.96
(A)	20.31	10.56	.723	.728	.736	.143	26.71	50.01
(B)	20.31	10.56	.502	.516	.516	.131	36.07	61.66
(C)	20.31	10.56	.221			.012	5.01	21.82
(A)	25.37	15.62	.807	.832	.835	.24	32.12	49.95
(B)	25.37	15.62	.614	.642	.639	.204	38.35	60.38
(C)	25.37	15.62	.193			.036	11.93	13.33
(A)	30.45	20.7	.904	.942	.944	.322	33.43	52.82
(B)	30.45	20.7	.767	.825	.809	.323	41.49	53.09
(C)	30.45	20.7	.137			-.001	-15.49	46.36
(A)	32.99	23.24	.956	1.002	1.002	.367	34.36	52.31
(A)	35.52	25.77	.996	1.054	1.051	.418	35.21	52.07
(B)	35.52	25.77	.776	.856	.829	.306	43.94	58.79
(C)	35.52	25.77	.22			.032	1.75	22.37
(A)	37.81	28.06	.724	.842	.788	.441	37.48	44.43
(B)	37.81	28.06	.488	.633	.548	.403	50.02	54.16
(C)	37.81	28.06	.236			.038	4.26	15.22

REYNOLDS NO. = 1.23000E+06

SKEG ANGLE, BETA(DEG.) = -.25 (WITHOUT TRANSITION STRIP)

	AA	AD	CL	CN	CY	CD	CPC	CPS
(A)	-.27	-.02	-.028	-.028	-.028	.019	31.56	42.72
(A)	4.89	5.14	.179	.18	.179	.023	22.15	46.91
(A)	10.06	10.31	.396	.398	.396	.044	25.77	47.36
(A)	12.64	12.89	.511	.514	.51	.07	28.85	47.56
(A)	15.22	15.47	.608	.612	.608	.096	30.86	47.16
(A)	20.23	20.48	.625	.638	.625	.148	32.11	52.26
(A)	22.89	23.14	.83	.84	.829	.195	33.28	49.03
(A)	27.35	27.6	.782	.81	.781	.251	34.38	52.53
(A)	30.37	30.62	.806	.845	.804	.296	35.51	54.11
(A)	33.41	33.66	.853	.905	.851	.351	36.88	54.07

REYNOLDS NO. = 860000

ALL-MOVABLE RUDDER

	AA	AD	CL	CN	CY	CD	CPC	CPS
(A)	-4.41	-.16	-.21	-.212	-.212	.03	18.09	46.05
(A)	-2.34	-.09	-.114	-.115	-.115	.023	13.86	44.86
(A)	-1.3	-.05	-.06	-.061	-.061	.023	19.23	47.77
(A)	-.26	-.01	-.01	-.01	-.01	.019	24.1	67.99
(A)	.78	.03	.04	.04	.041	.019	15.61	36.37
(A)	1.82	.07	.089	.089	.089	.017	18.32	41.16
(A)	2.86	.11	.137	.138	.138	.02	15.95	43.83
(A)	4.93	.18	.235	.236	.236	.023	16.42	44.36
(A)	7	.25	.329	.33	.33	.028	18.01	44.63
(A)	10.12	.37	.477	.477	.477	.041	17.87	45.68
(A)	15.31	.56	.727	.723	.722	.082	19.36	46.16
(A)	20.45	.7	.907	.913	.911	.181	23.19	44.6
(A)	22.42	.67	.865	.888	.887	.233	30.95	45.47
(A)	25.36	.61	.785	.839	.837	.303	30.53	45.93
(A)	27.74	.49	.641	.717	.715	.321	32.39	51.89

REYNOLDS NO. = 1.23000E+06

ALL-MOVABLE RUDDER

	AA	AD	CL	CN	CY	CD	CPC	CPS
(A)	-.26	-.01	-.016	-.016	-.016	.02	34.36	18.08
(A)	4.93	.18	.23	.231	.231	.022	15.98	44.11
(A)	10.11	.36	.472	.472	.472	.042	17.52	45.64
(A)	12.71	.46	.598	.597	.596	.061	18.38	45.8
(A)	15.31	.56	.726	.723	.722	.085	19.61	46.221
(A)	17.89	.64	.835	.832	.832	.122	21.12	46.69

AA=RUDDER ANGLE, ALPHA(DEG.), AD=RUDDER ANGLE, DELTA(DEG.)
CL=LIFT COEFFICIENT, CN=RUDDER NORMAL COEFFICIENT
CY=SHIP NORMAL COEFFIENT, CD=DRAG COEFFICIENT
CPC=C OF P CHORD(%C), CPS=C OF P SPAN(%S)
ALL COEFFICIENTS BASED ON TOTAL AREA OF RUDDER PLUS SKEG.
(A)=RUDDER PLUS SKEG, (B)=RUDDER ALONE, (C)=SKEG ALONE

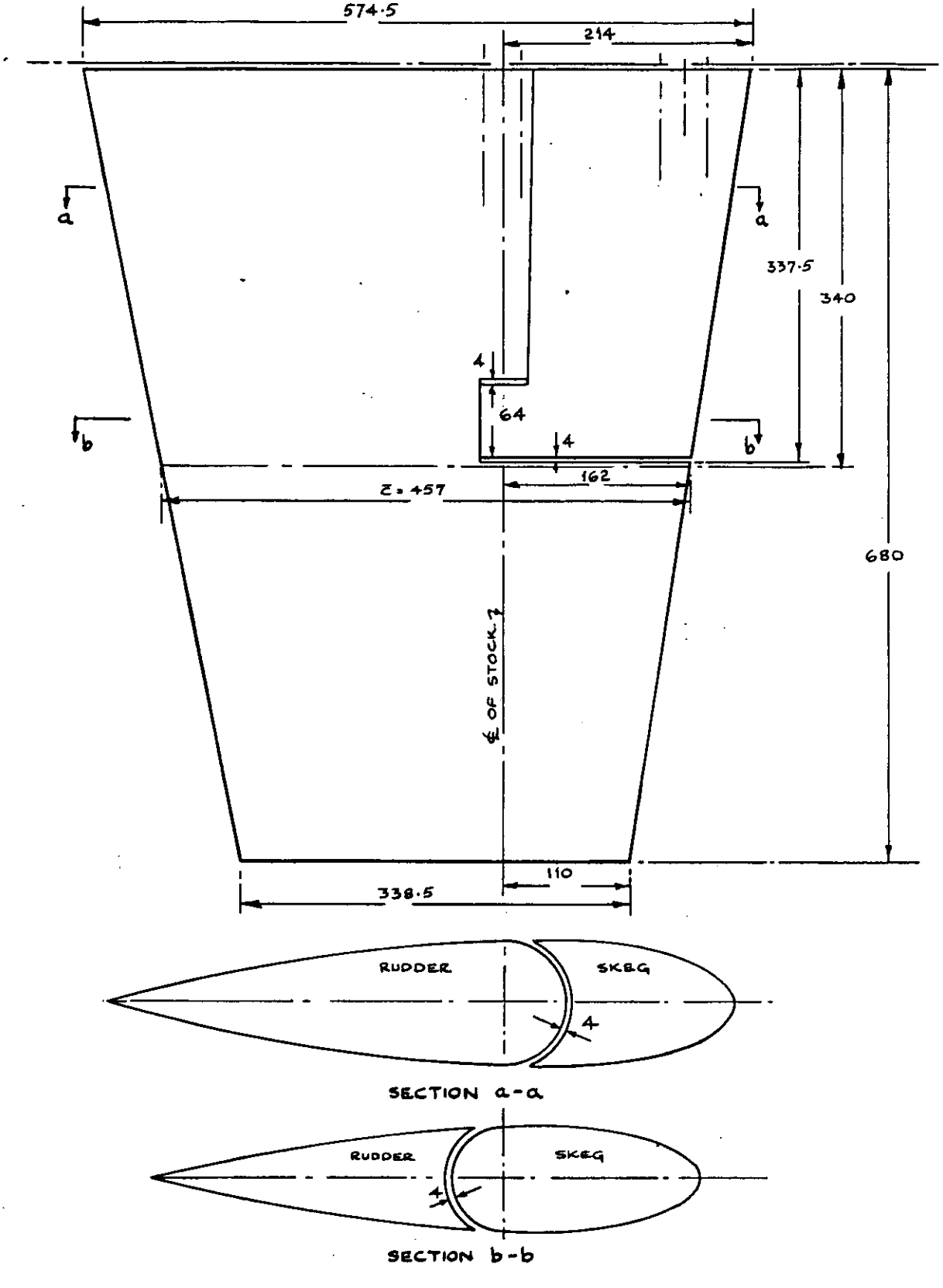

Fig. 1 MODEL RUDDER DIMENSIONS

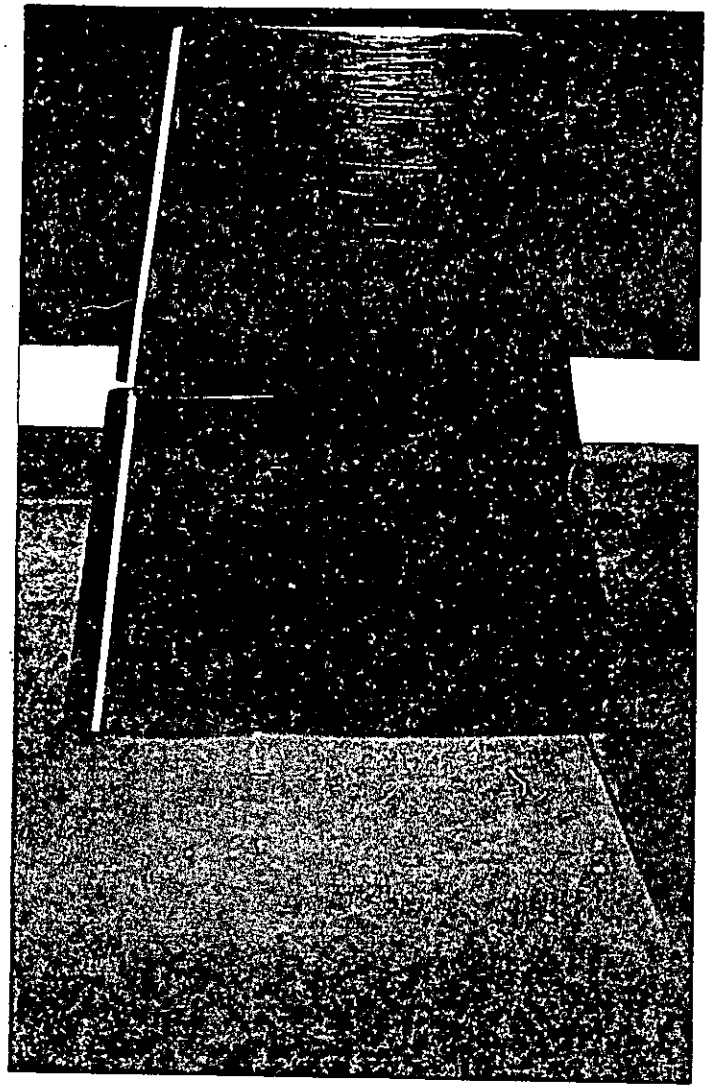

Fig. 2a SKEG RUDDER IN WIND TUNNEL

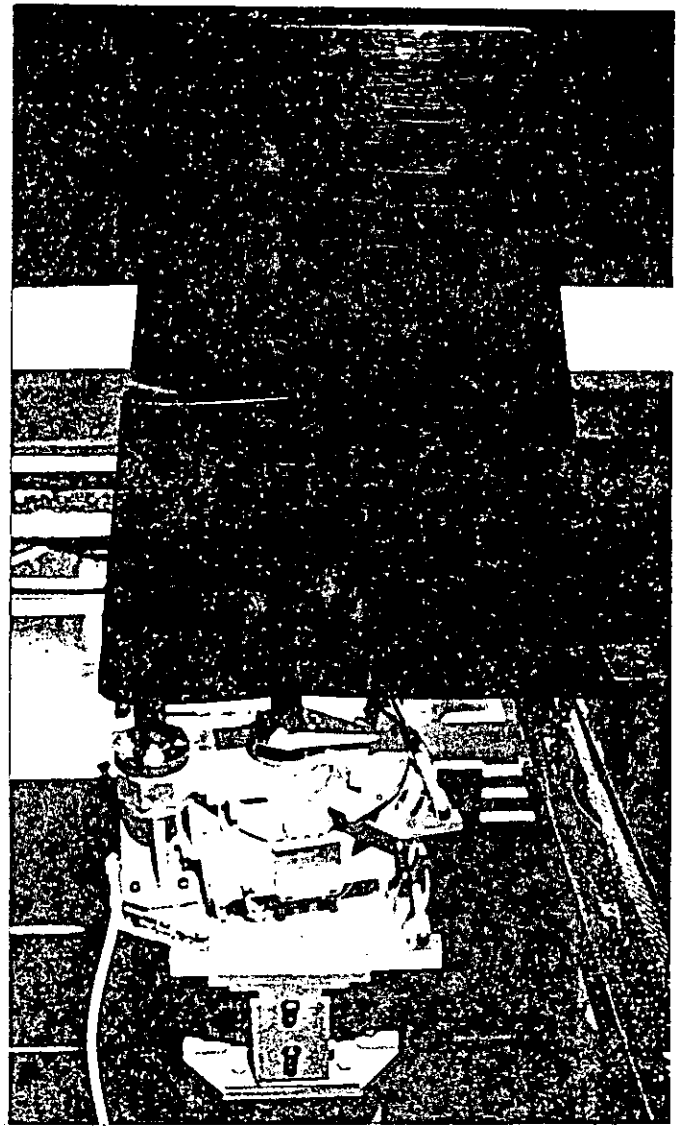

Fig. 2b SKEG RUDDER IN WIND TUNNEL
(Tunnel floor removed to show dynamometer)

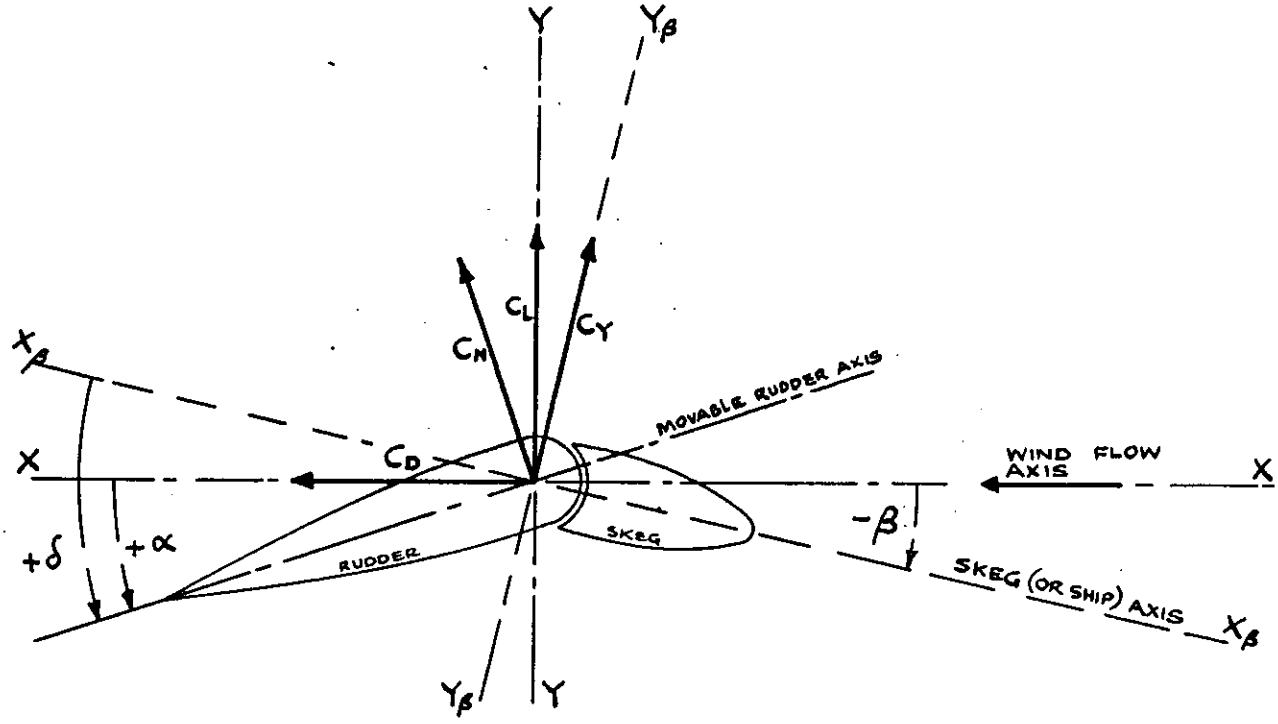

Fig. 3 NOTATION OF ANGLES AND COEFFICIENTS

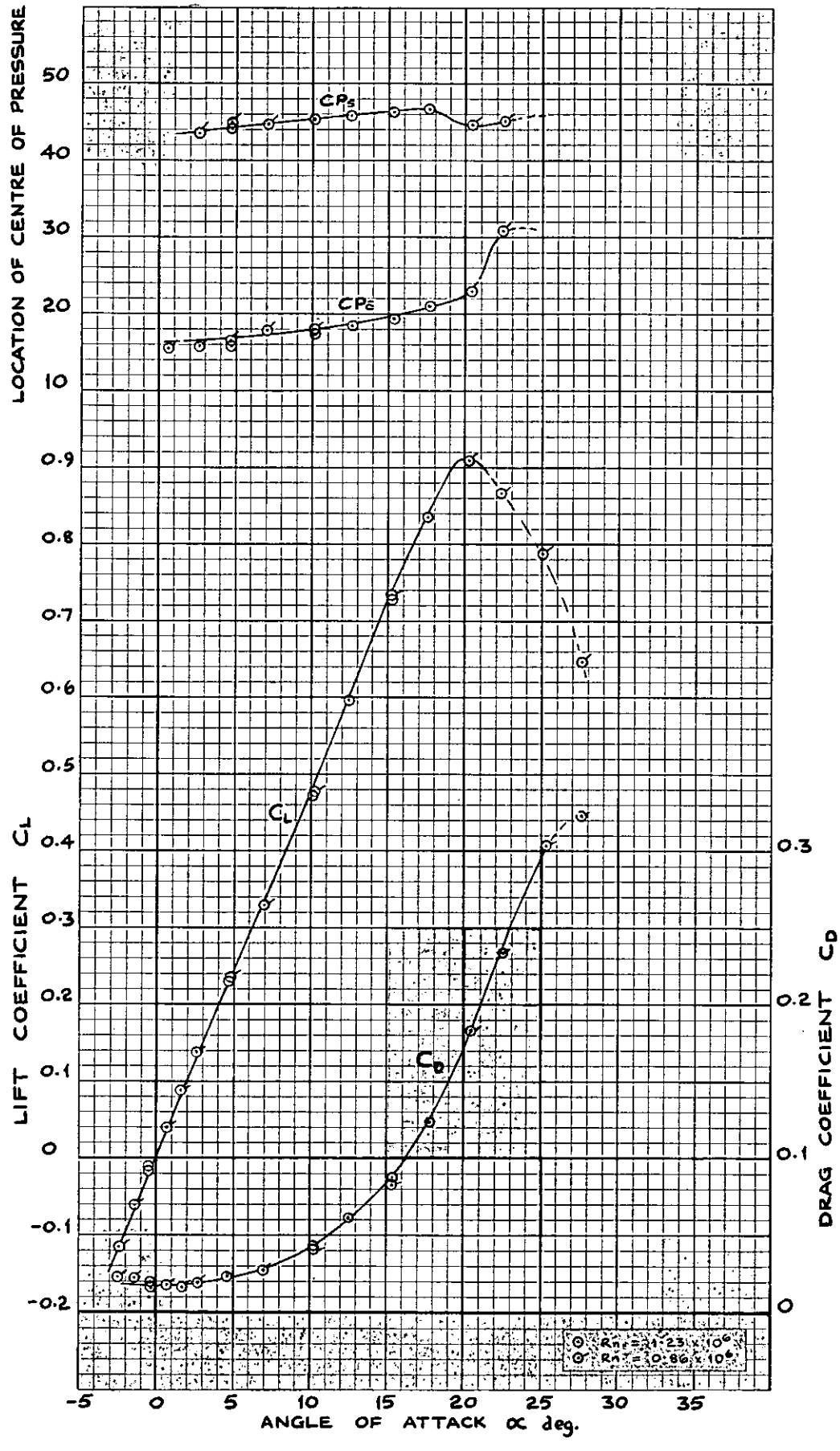

Fig. 4 LIFT, DRAG AND CENTRE OF PRESSURE CHARACTERISTICS FOR ALL-MOVABLE RUDDER

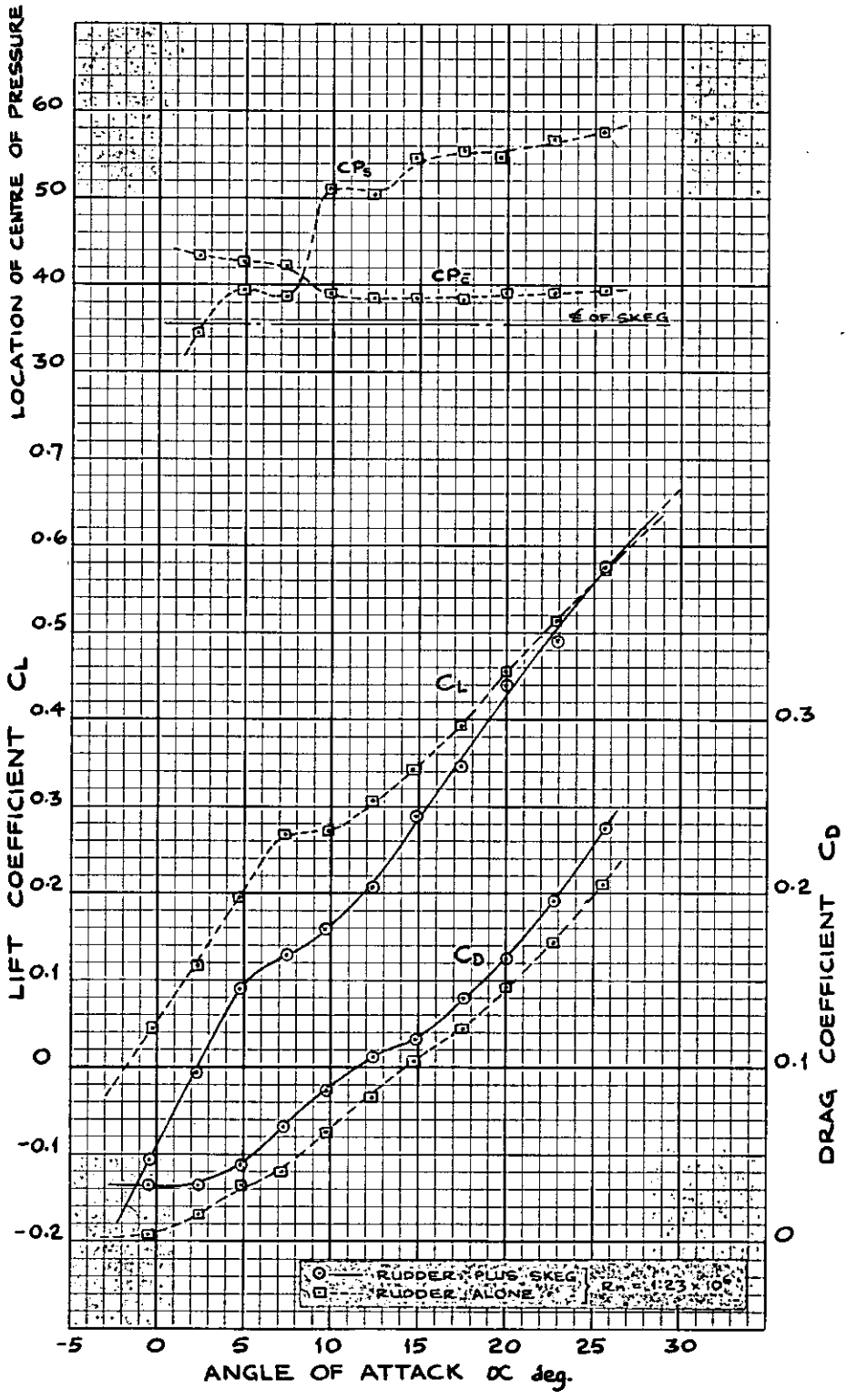

SKEG ANGLE $\beta = -15.25°$

Fig. 5a LIFT, DRAG AND CENTRE OF PRESSURE CHARACTERISTICS FOR SKEG RUDDER

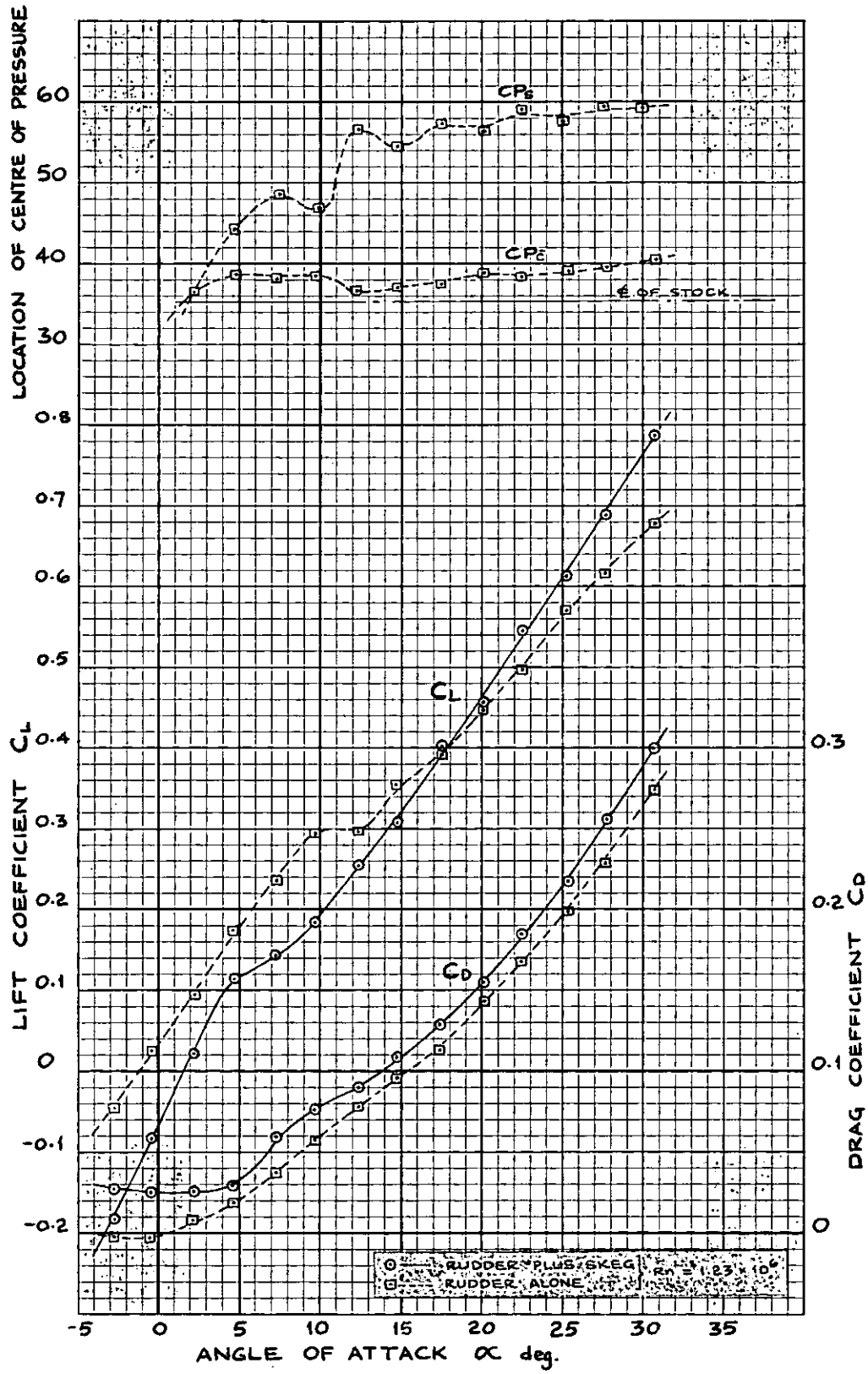

SKEG ANGLE $\beta = -10.25°$

Fig. 5b LIFT, DRAG AND CENTRE OF PRESSURE CHARACTERISTICS FOR SKEG RUDDER

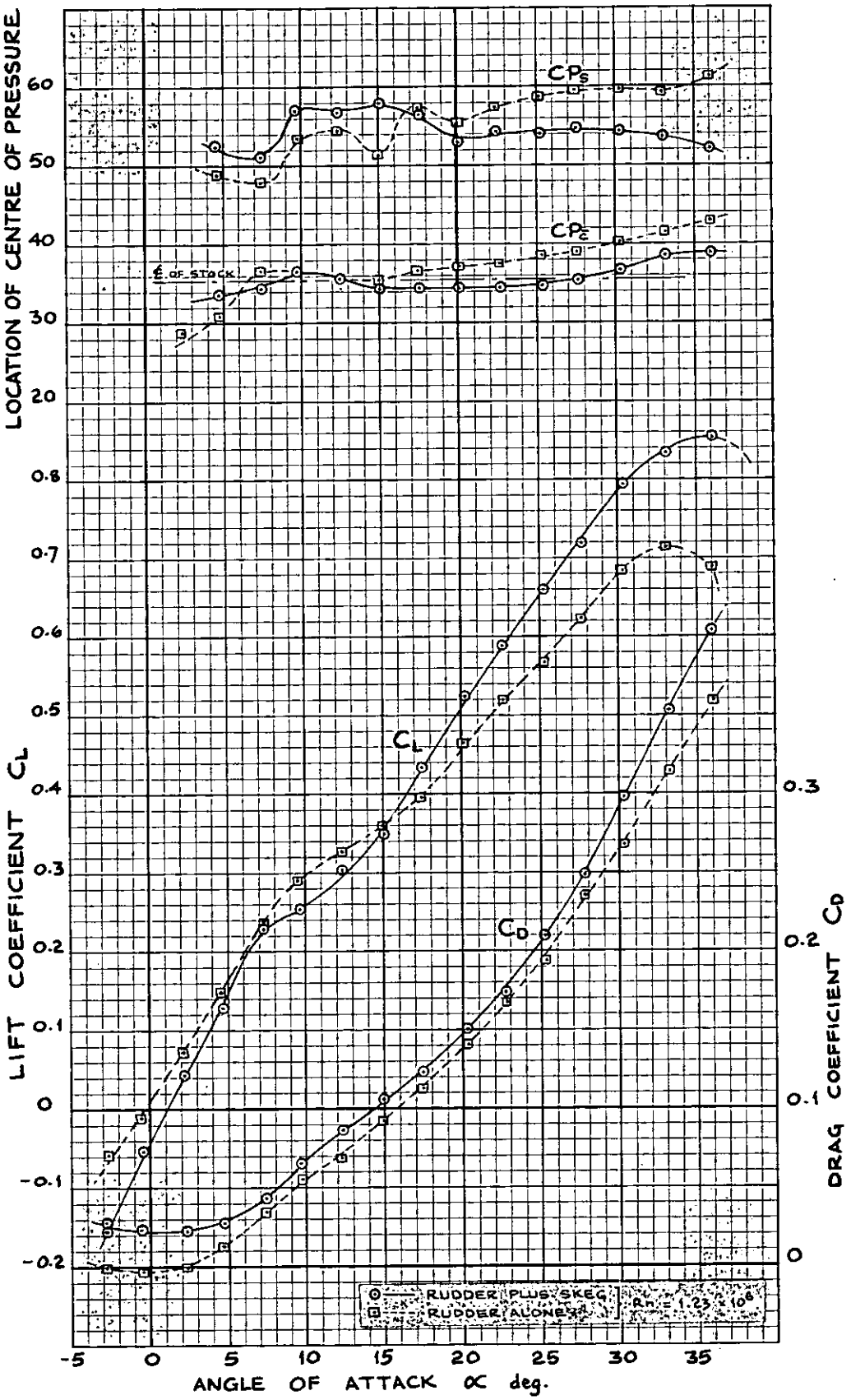

SKEG ANGLE $\beta = -5.25°$

Fig. 5c LIFT, DRAG AND CENTRE OF PRESSURE CHARACTERISTICS FOR SKEG RUDDER

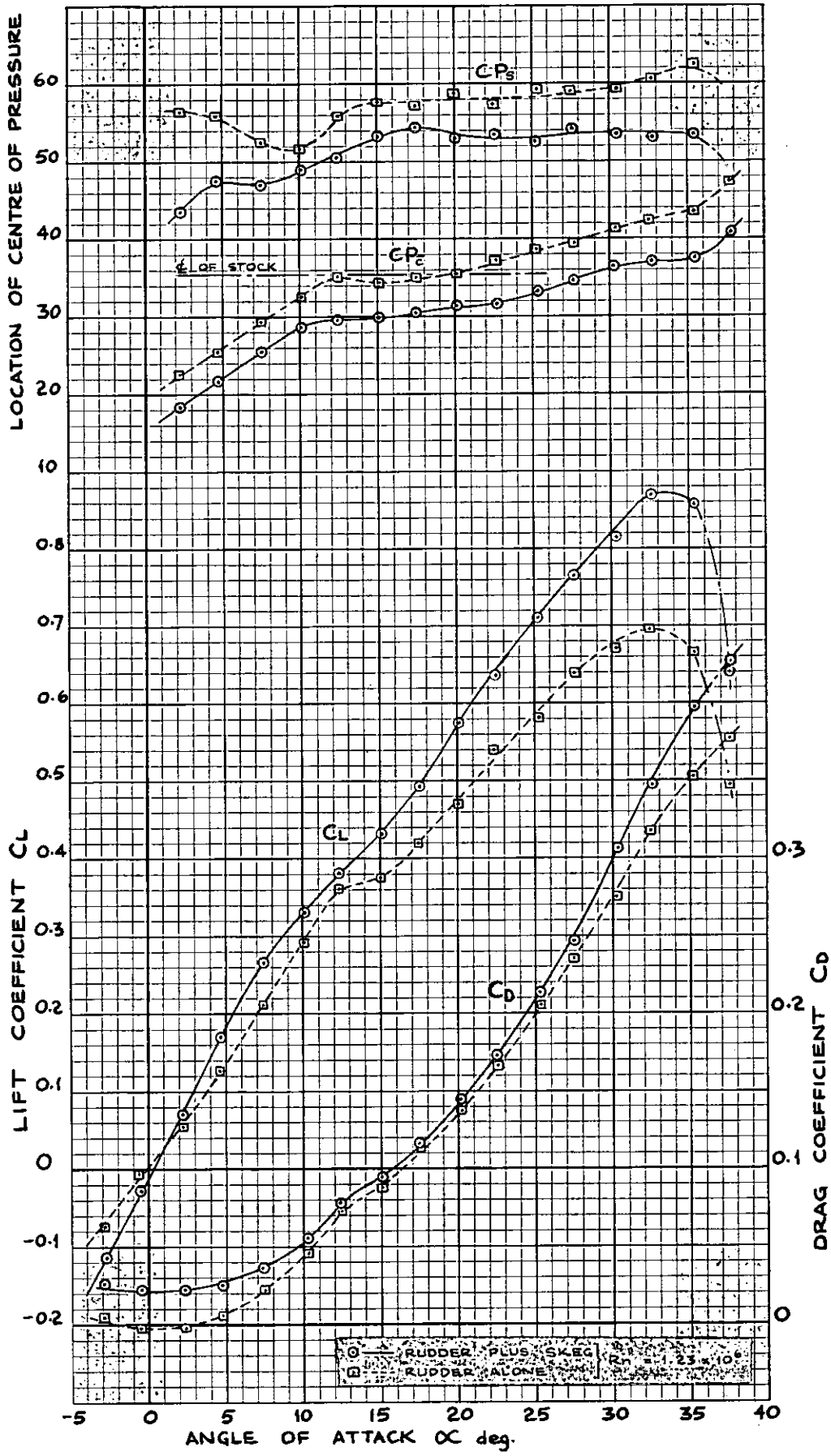

SKEG ANGLE $\beta = -0.25°$

Fig. 5d LIFT, DRAG AND CENTRE OF PRESSURE CHARACTERISTICS FOR SKEG RUDDER

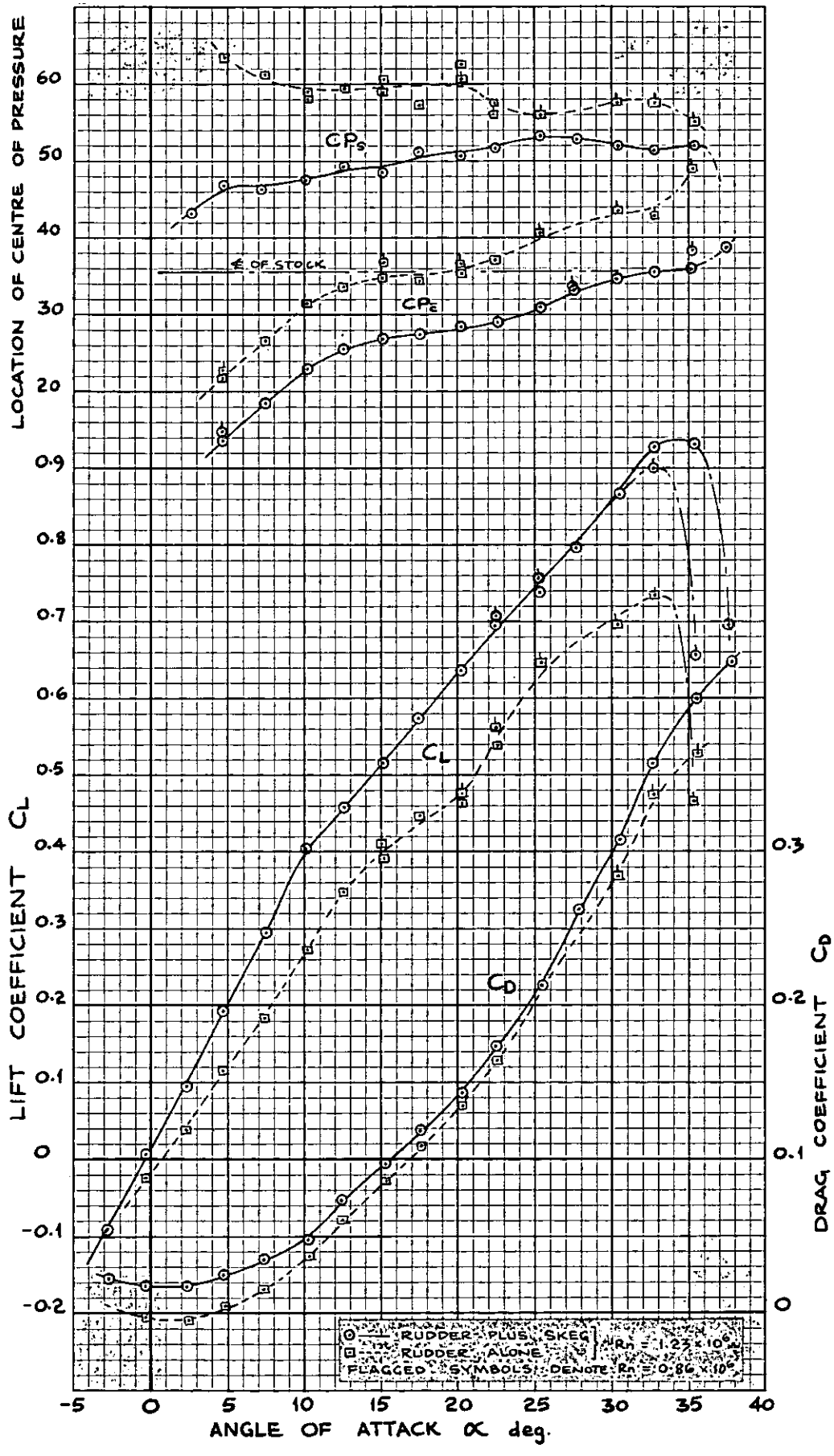

SKEG ANGLE $\beta = +4.75°$

Fig. 5e LIFT, DRAG AND CENTRE OF PRESSURE CHARACTERISTICS FOR SKEG RUDDER

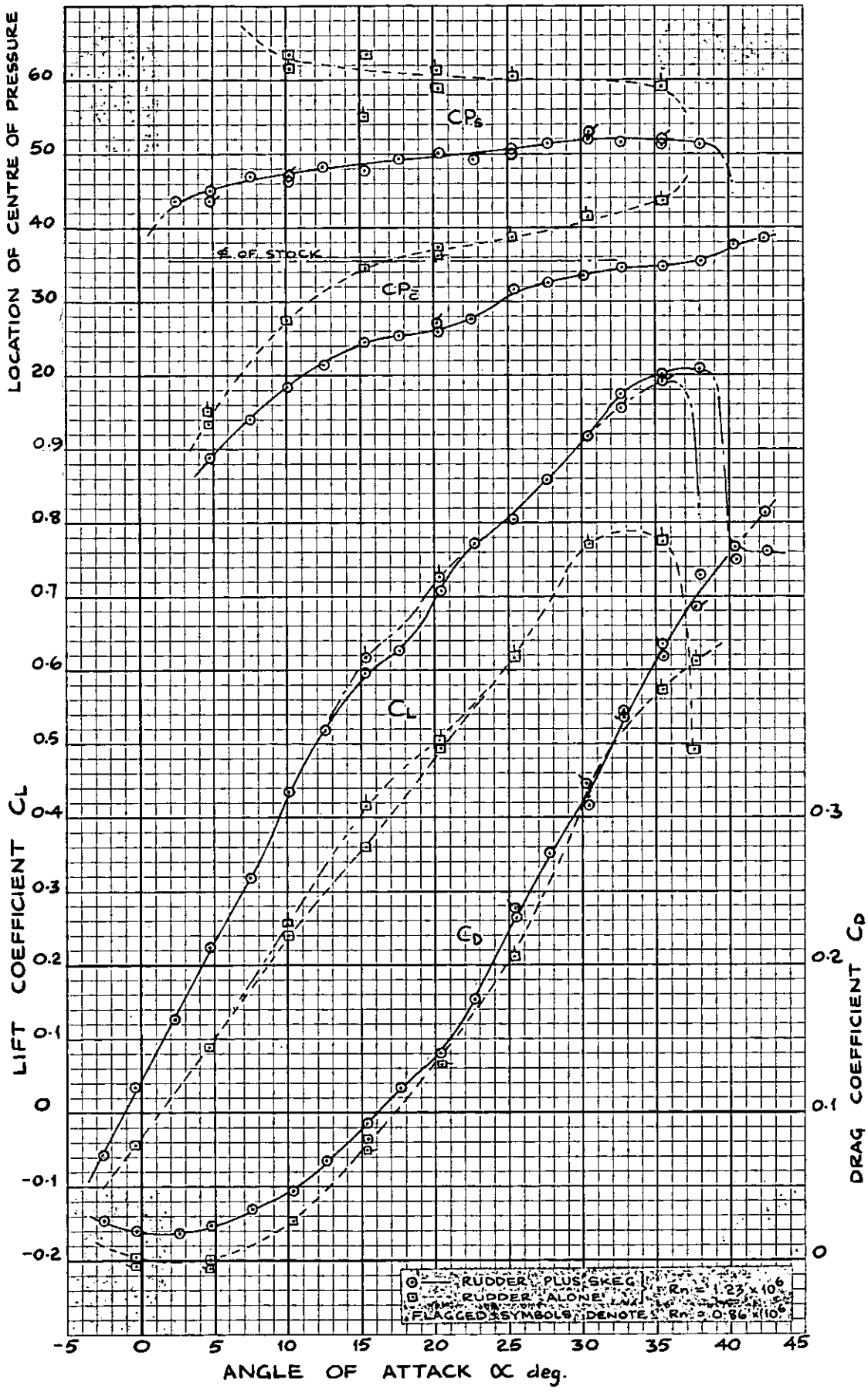

SKEG ANGLE $\beta = +9.75°$

Fig. 5f LIFT, DRAG AND CENTRE OF PRESSURE CHARACTERISTICS FOR SKEG RUDDER

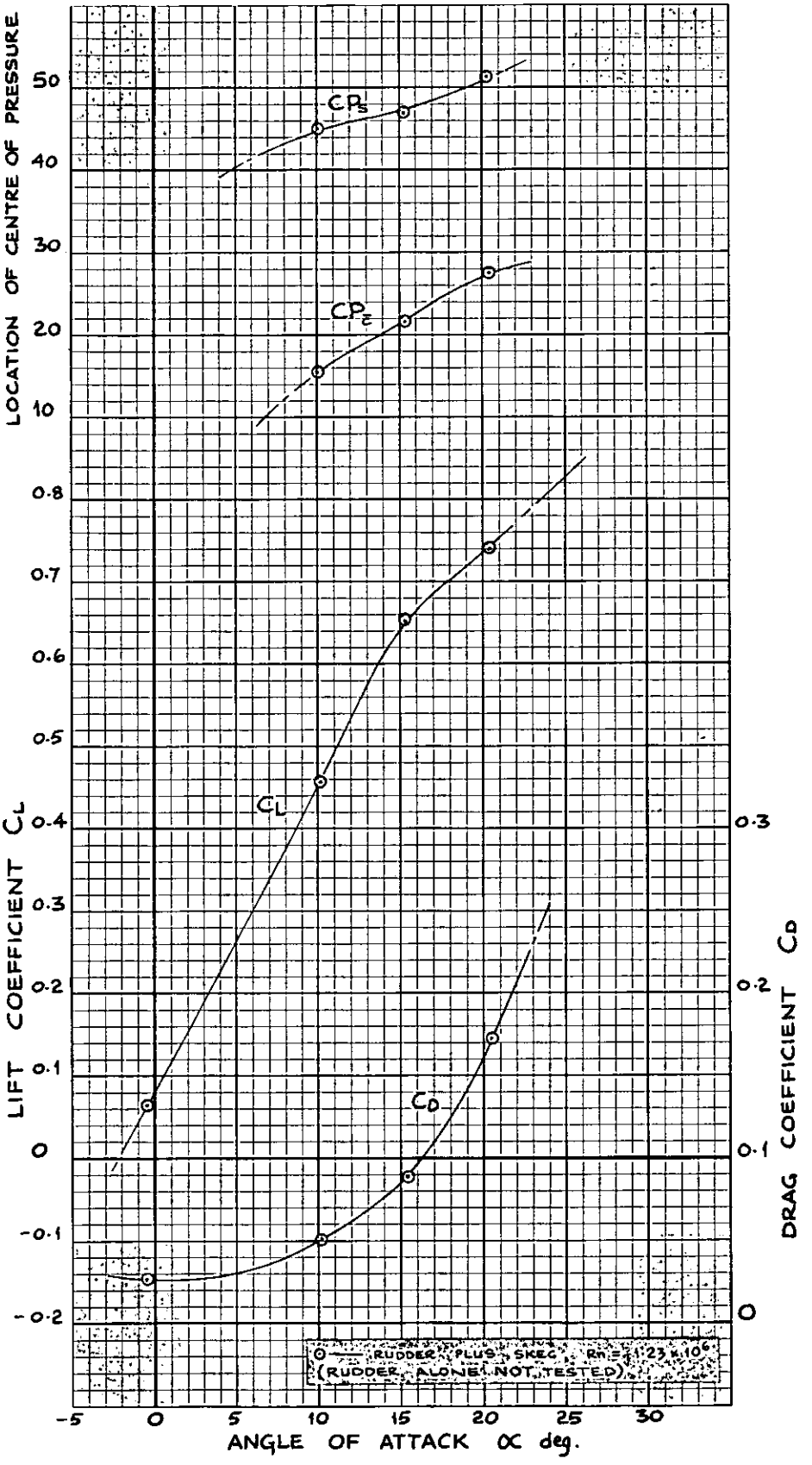

SKEG ANGLE $\beta = +14.75°$

Fig. 58 LIFT, DRAG AND CENTRE OF PRESSURE CHARACTERISTICS FOR SKEG RUDDER

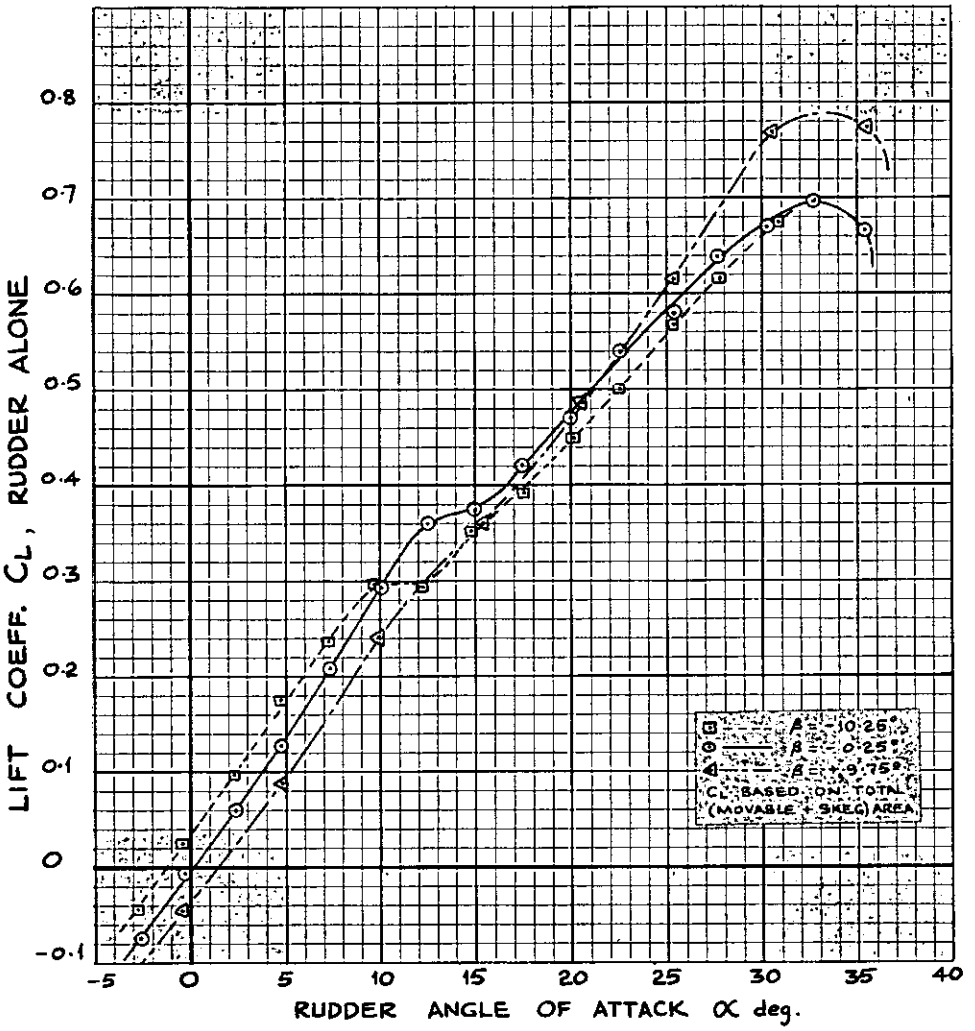

Fig. 6 SELECTED LIFT CHARACTERISTICS FOR RUDDER ALONE

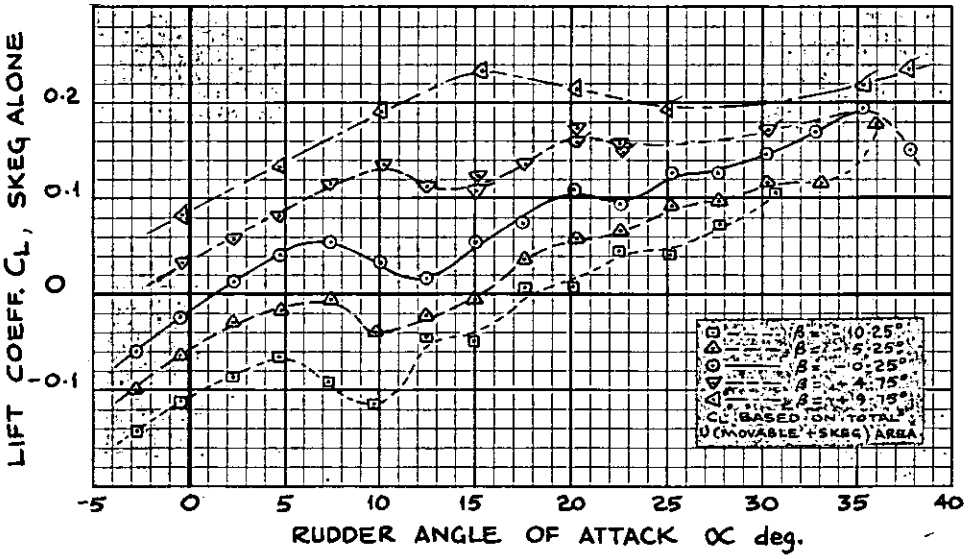

Fig. 7 LIFT CHARACTERISTICS FOR SKEG ALONE FOR VARIATION IN RUDDER ANGLE OF ATTACK α

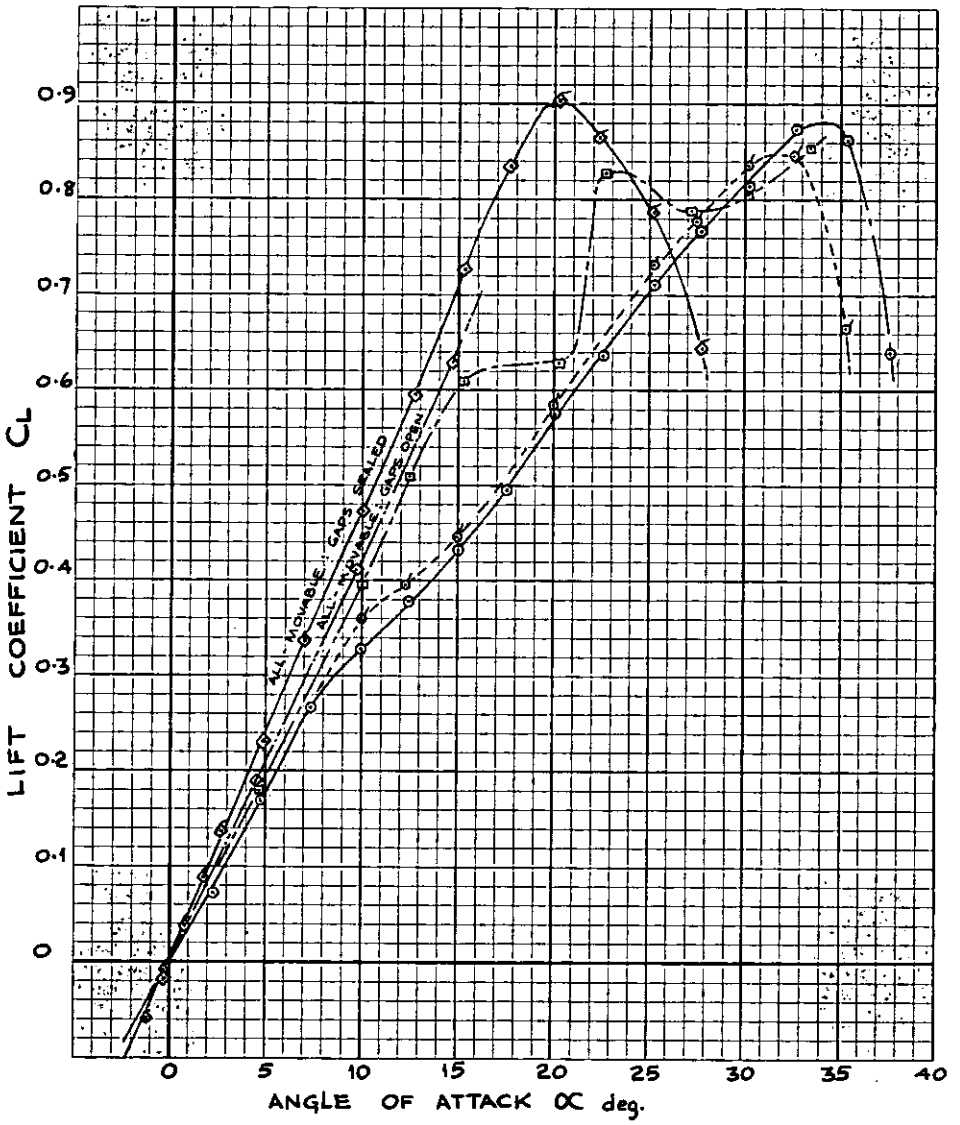

◇—— ALL-MOVABLE
⊙—— SKEG RUDDER, $\beta = 0$
⊡--- " " " ", WITHOUT TRANSITION STRIP
} $Rn = 1{\cdot}23 \times 10^6$

FLAGGED SYMBOLS DENOTE REDUCED $Rn = 0{\cdot}86 \times 10^6$

Fig. 8 COMPARISON OF LIFT COEFFICIENT VERSUS ANGLE OF ATTACK FOR ALL-MOVABLE RUDDER AND SKEG RUDDER AT $\beta = 0$, REDUCED Rn, AND WITHOUT TRANSITION STRIP

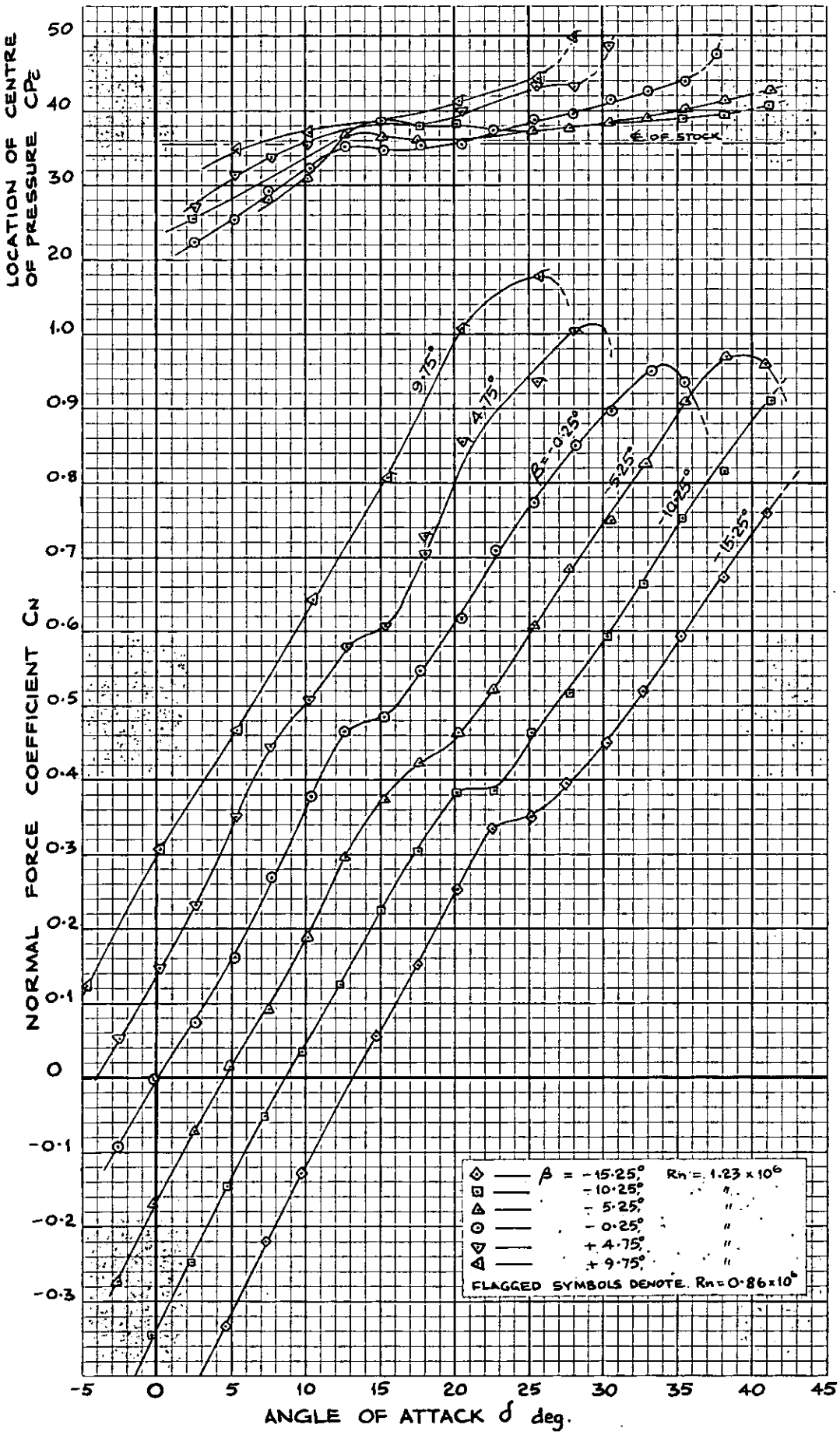

Fig. 9 RUDDER NORMAL FORCE COEFFICIENT AND CENTRE OF PRESSURE CHARACTERISTICS FOR SKEG RUDDER (COEFFICIENTS FOR RUDDER ALONE AND BASED ON MOVABLE AREA)

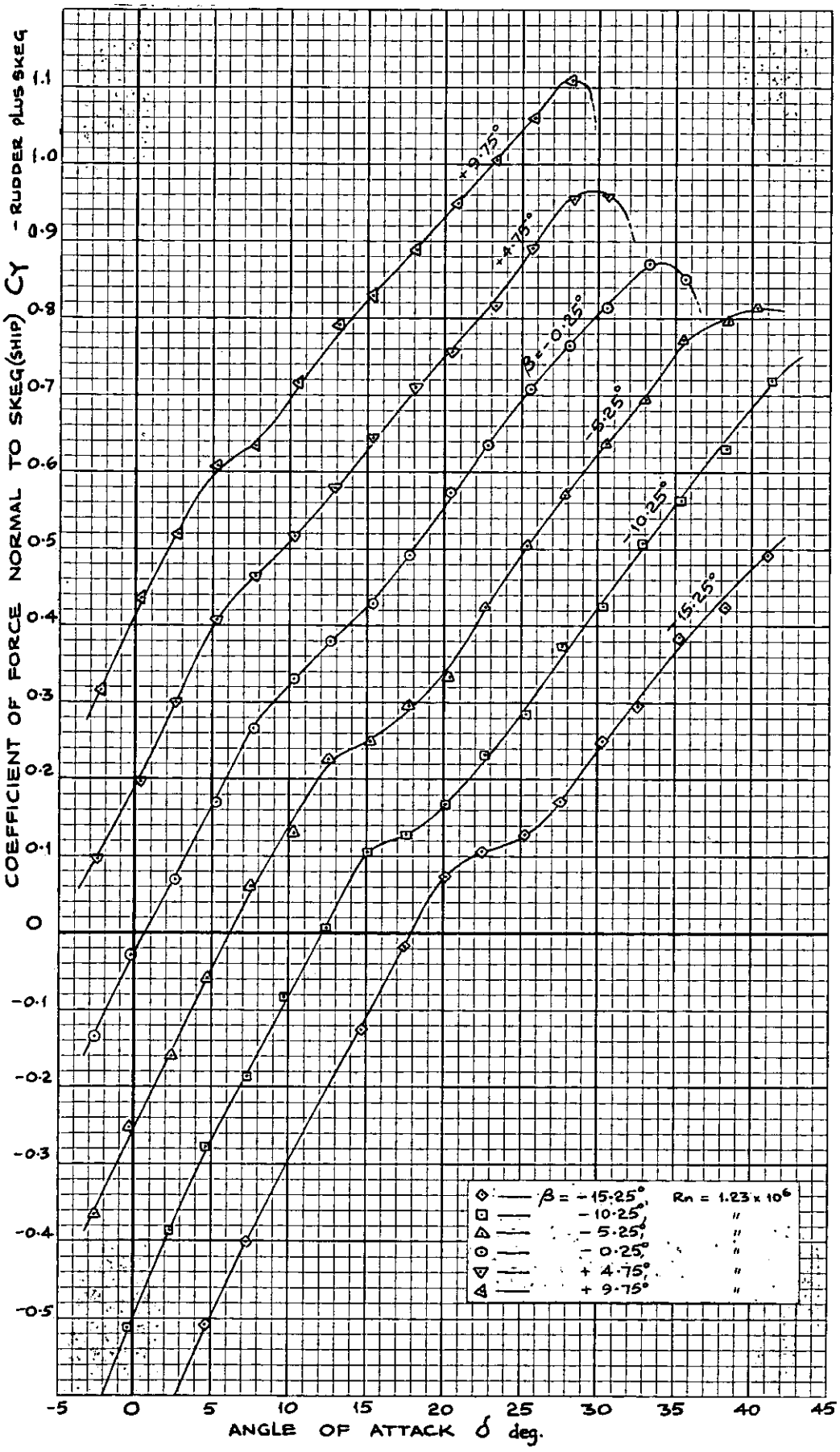

Fig. 10 SHIP NORMAL FORCE COEFFICIENT CHARACTERISTICS FOR RUDDER PLUS SKEG

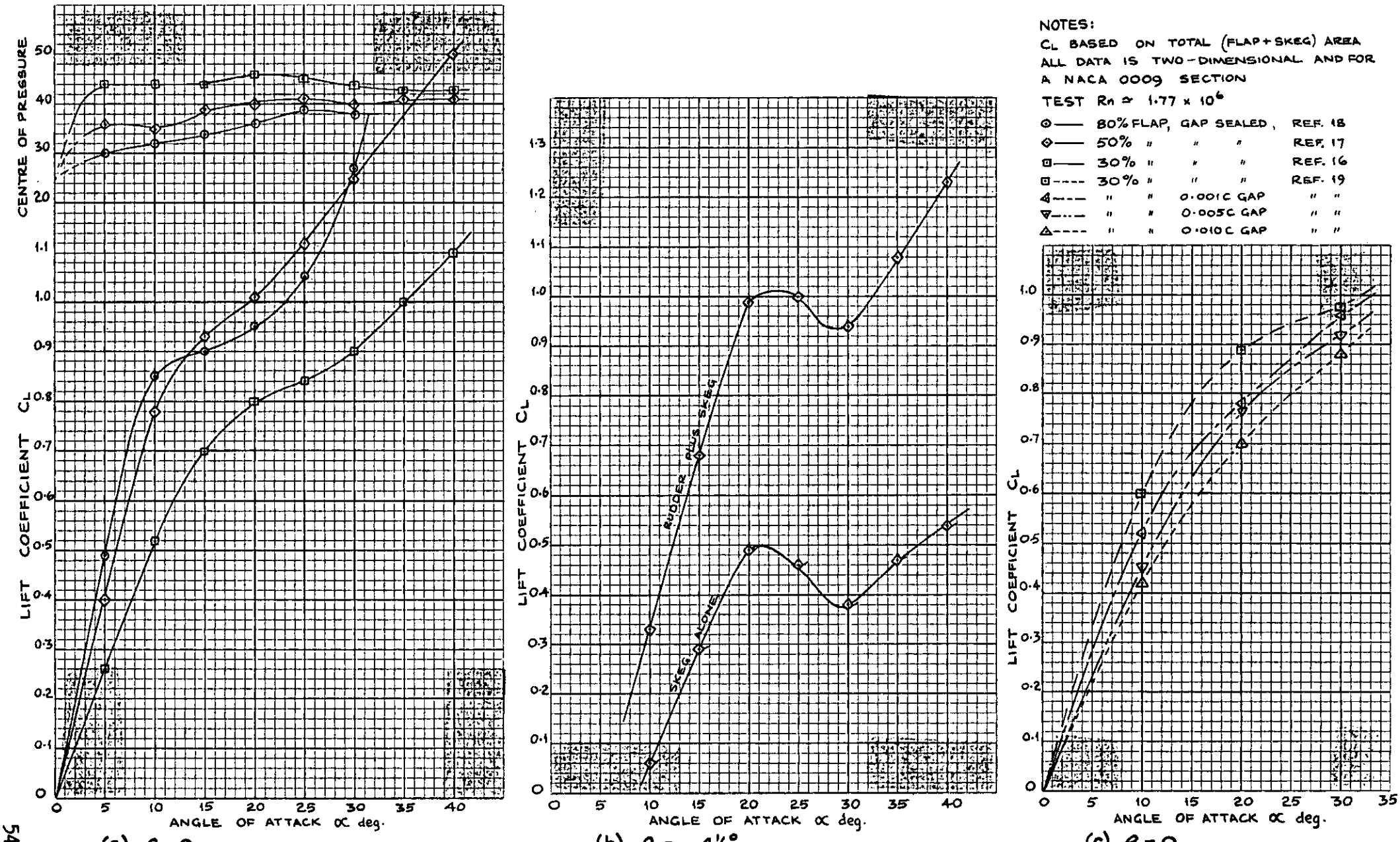

Fig. 11 SOME TWO-DIMENSIONAL SECTION DATA FOR FLAPPED AEROFOILS — DERIVED FROM REFS. 16, 17, 18, 19

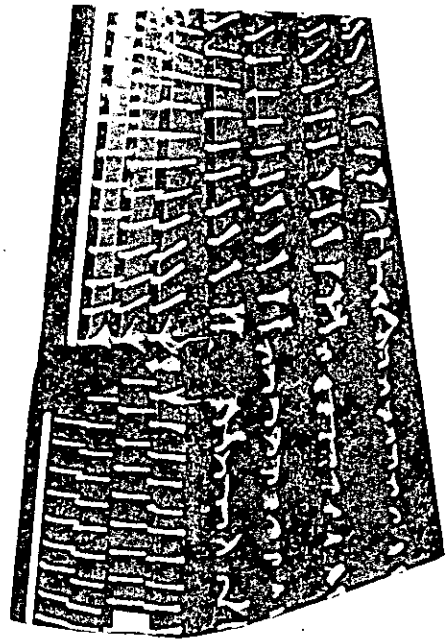

$\beta = -5°$
$\delta = +30°$ ($\alpha = 25°$)

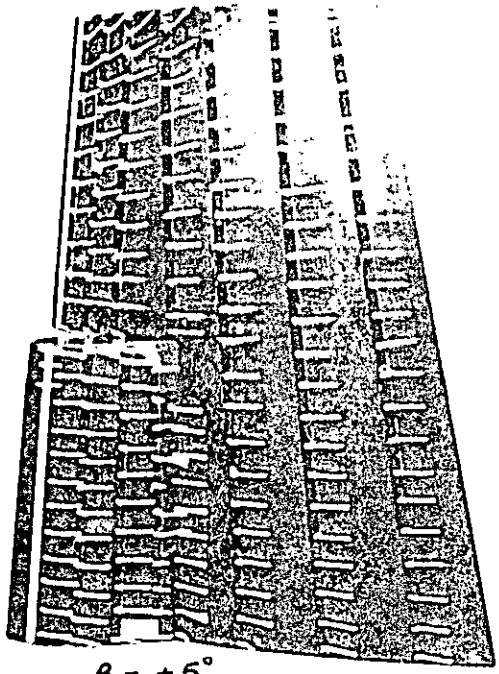

$\beta = +5°$
$\delta = -30°$ ($\alpha = -25°$)

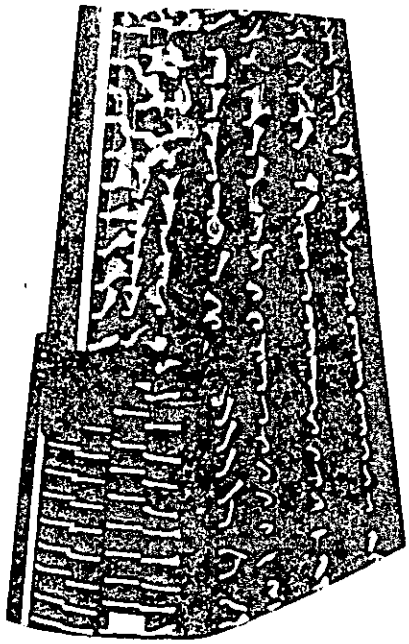

$\beta = -5°$
$\delta = +40°$ ($\alpha = 35°$)

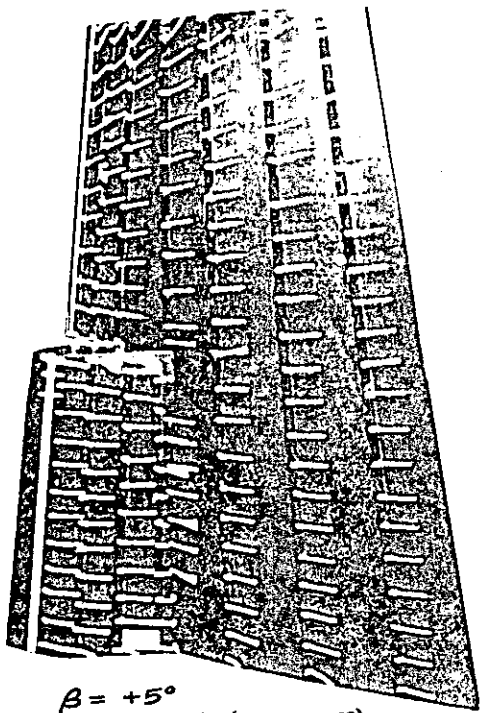

$\beta = +5°$
$\delta = -40°$ ($\alpha = -35°$)

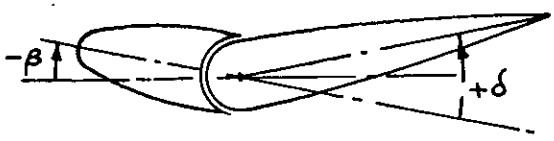

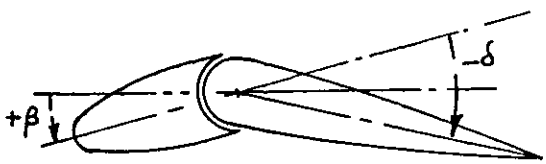

Fig. 12c FLOW PATTERNS OVER RUDDER

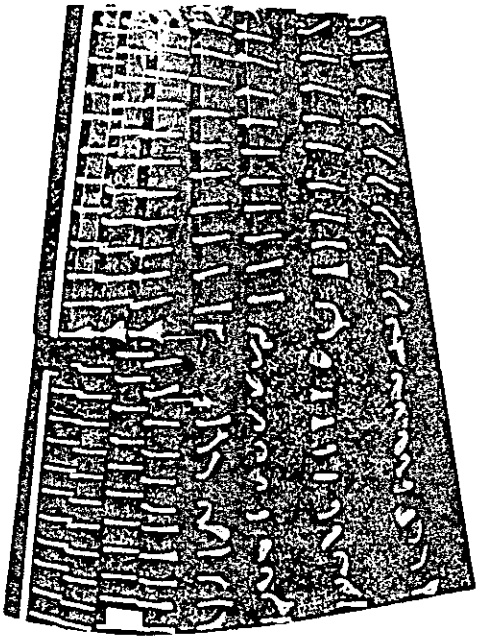

$\beta = -5°$
$\delta = +15°$ $(\alpha = 10°)$

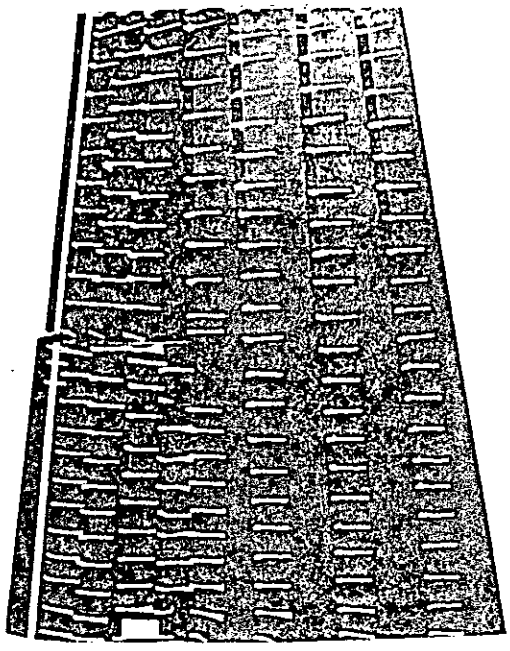

$\beta = +5°$
$\delta = -15°$ $(\alpha = -10°)$

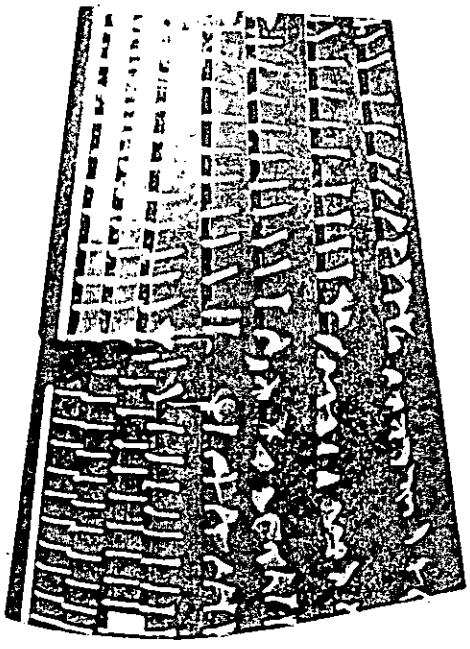

$\beta = -5°$
$\delta = +20°$ $(\alpha = 15°)$

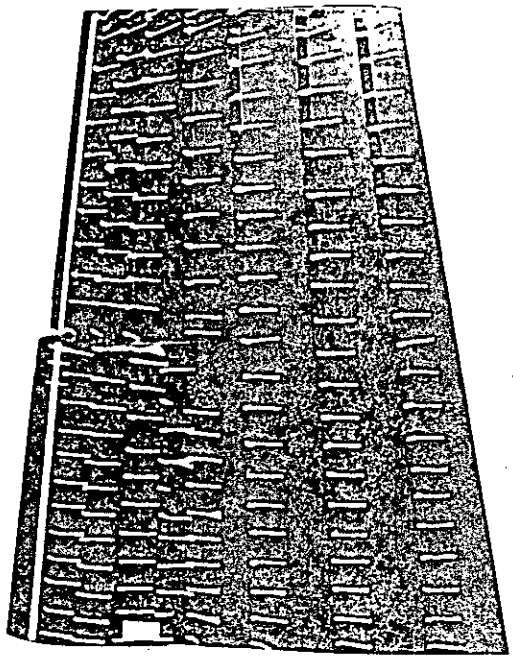

$\beta = +5°$
$\delta = -20°$ $(\alpha = -15°)$

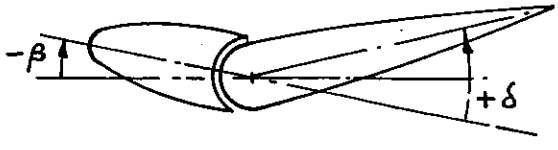

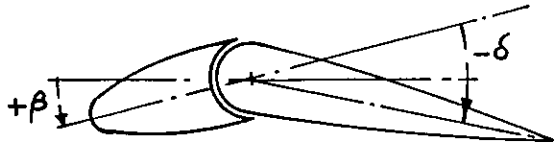

Fig. 12b FLOW PATTERNS OVER RUDDER

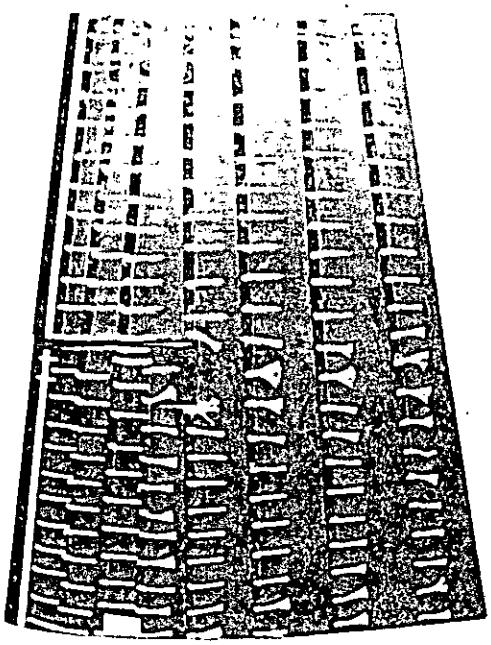

$\beta = -5°$
$\delta = +5°$ $(\alpha = 0°)$

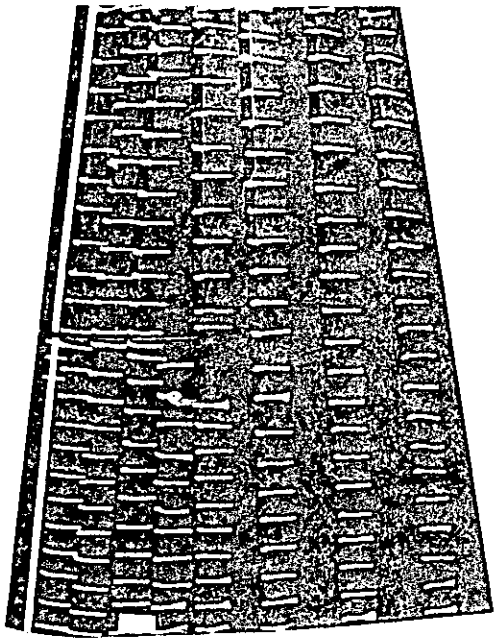

$\beta = +5°$
$\delta = -5°$ $(\alpha = 0°)$

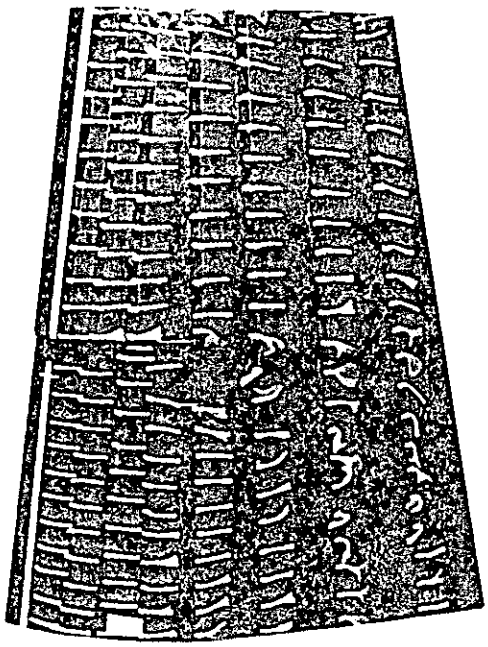

$\beta = -5°$
$\delta = +10°$ $(\alpha = 5°)$

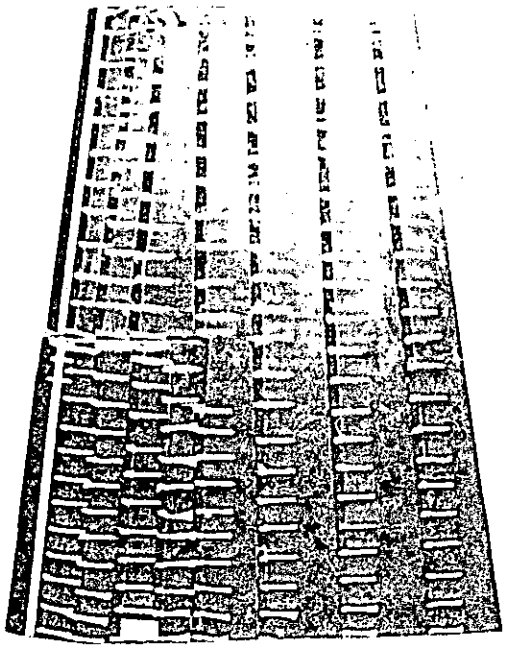

$\beta = +5°$
$\delta = -10°$ $(\alpha = -5°)$

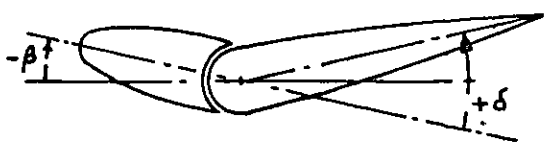

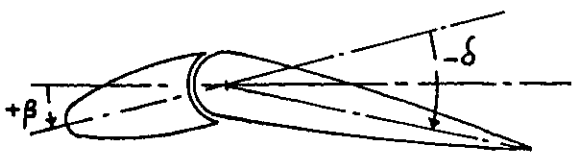

Fig. 12a FLOW PATTERNS OVER RUDDER

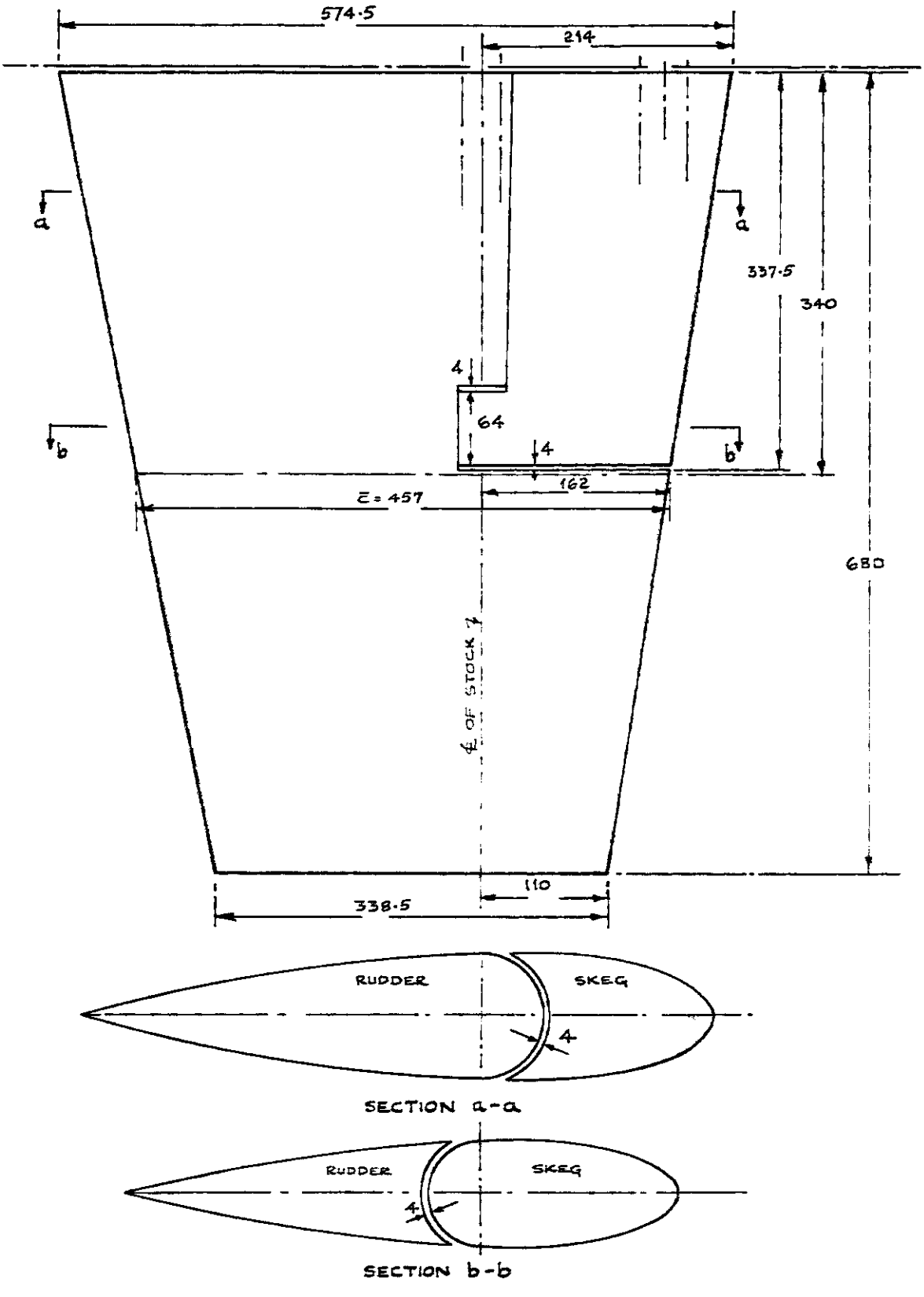

Fig. 1 MODEL RUDDER DIMENSIONS

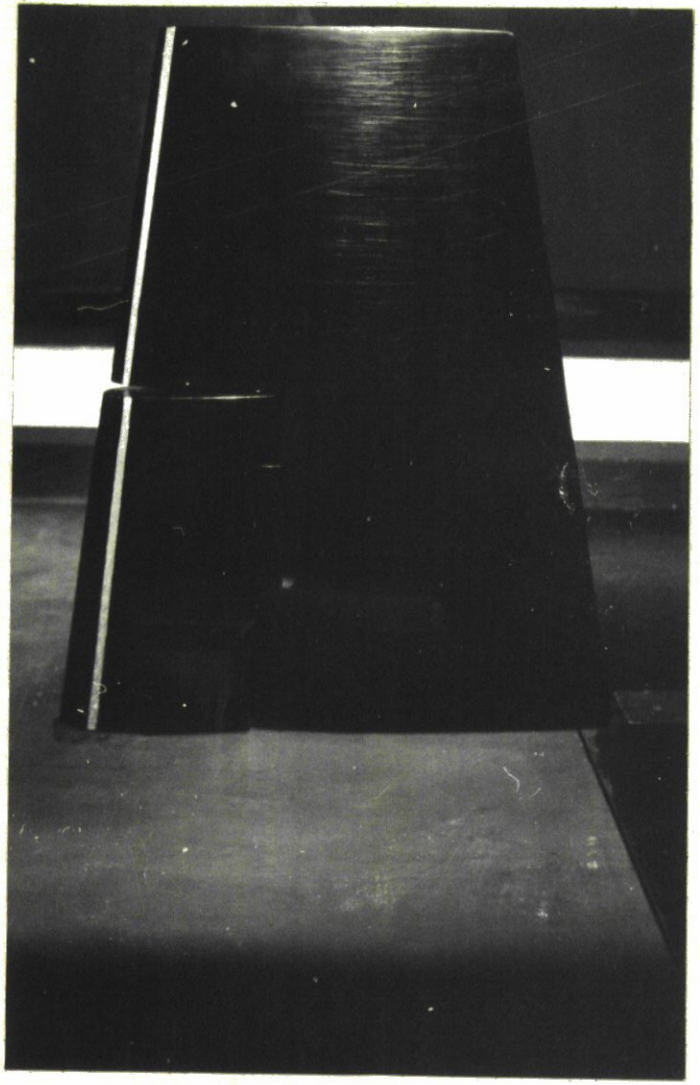

Fig. 2a SKEG RUDDER IN WIND TUNNEL

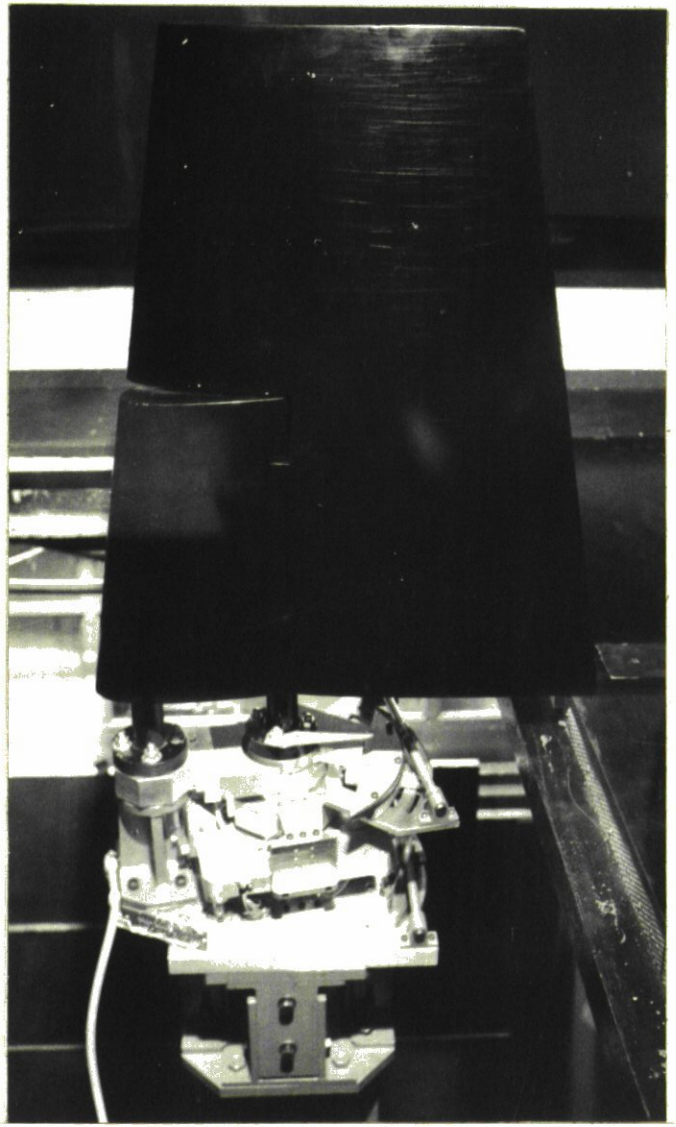

Fig. 2b SKEG RUDDER IN WIND TUNNEL
(Tunnel floor removed to show dynamometer)

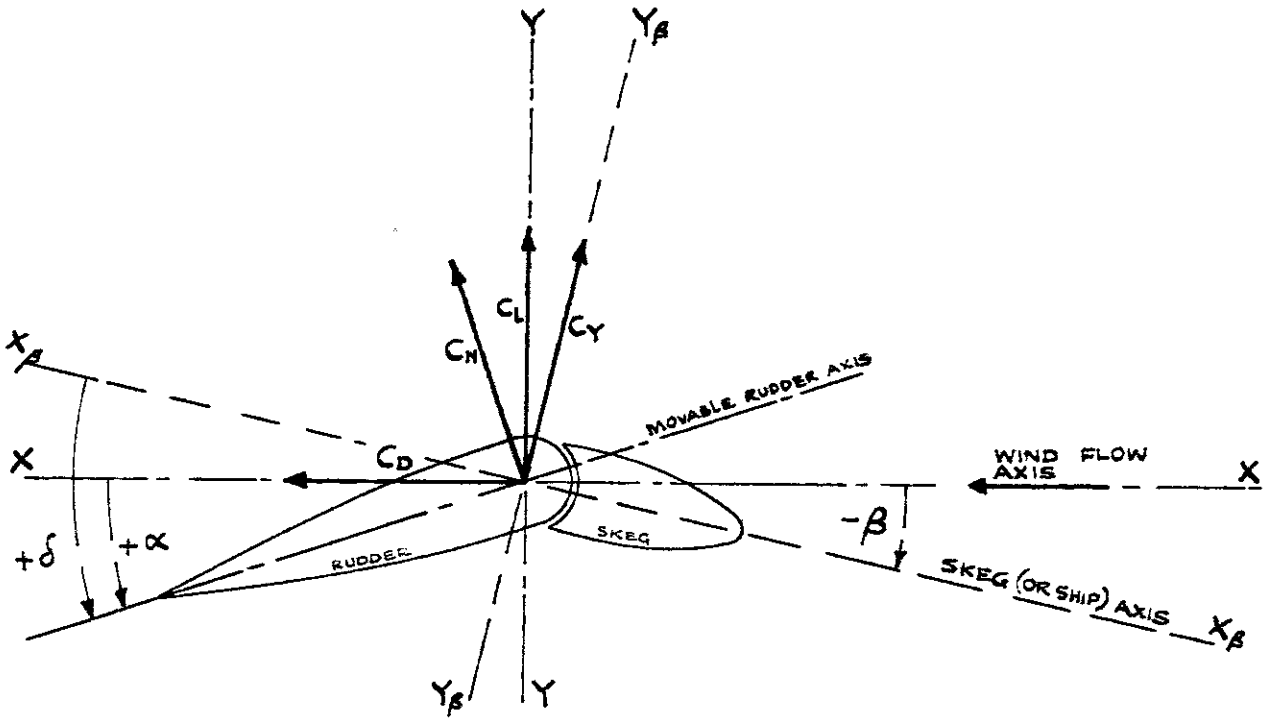

Fig. 3 NOTATION OF ANGLES AND COEFFICIENTS

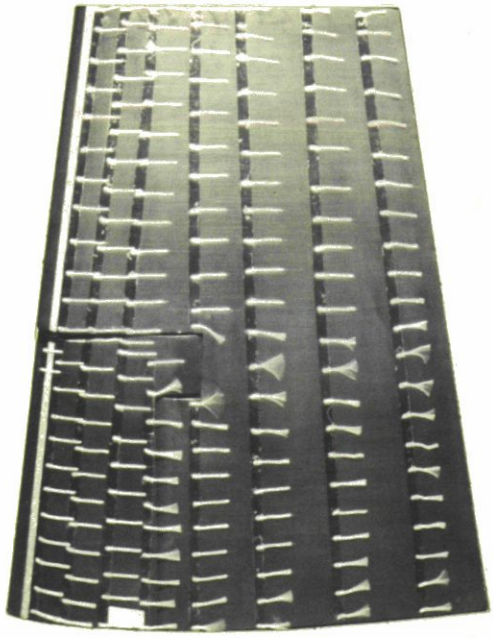

$\beta = -5°$
$\delta = +5°$ $(\alpha = 0°)$

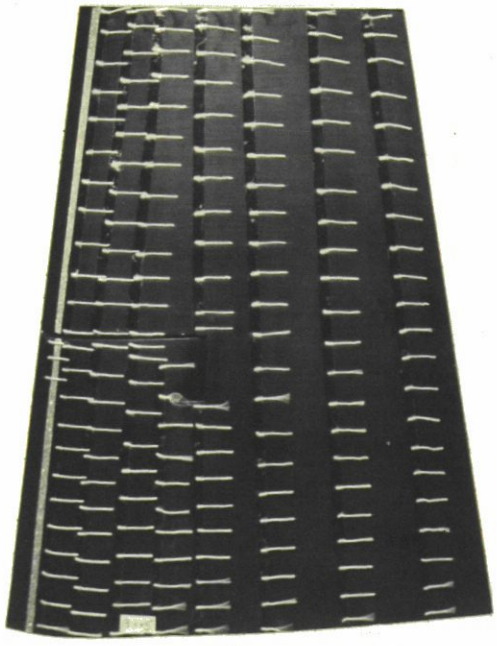

$\beta = +5°$
$\delta = -5°$ $(\alpha = 0°)$

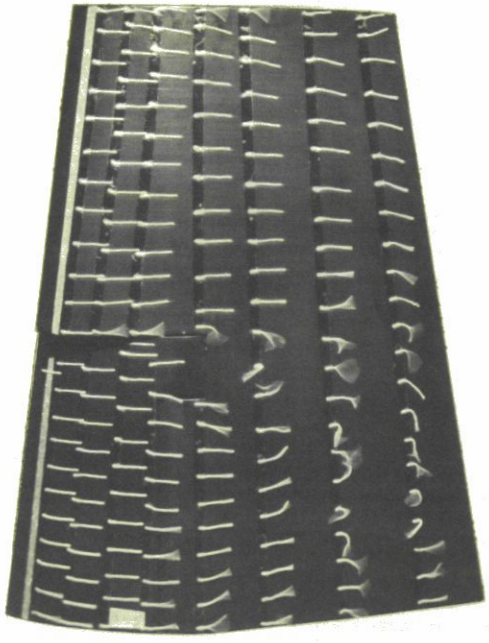

$\beta = -5°$
$\delta = +10°$ $(\alpha = 5°)$

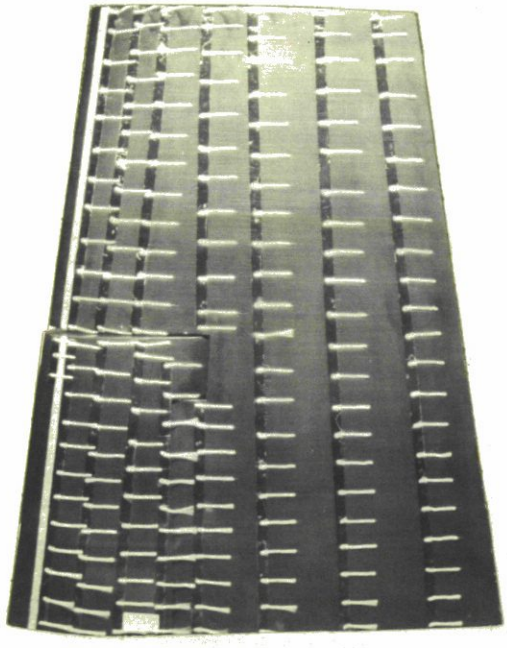

$\beta = +5°$
$\delta = -10°$ $(\alpha = -5°)$

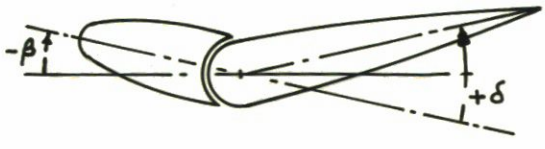

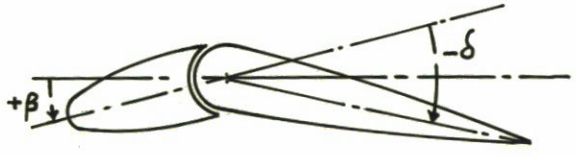

Fig. 12a FLOW PATTERNS OVER RUDDER

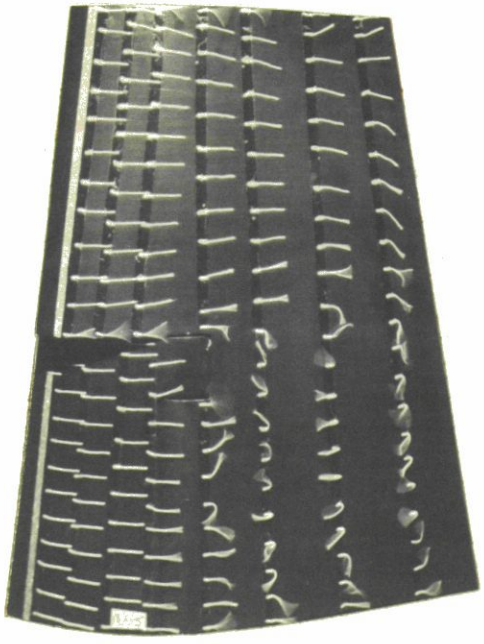

$\beta = -5°$
$\delta = +15°$ $(\alpha = 10°)$

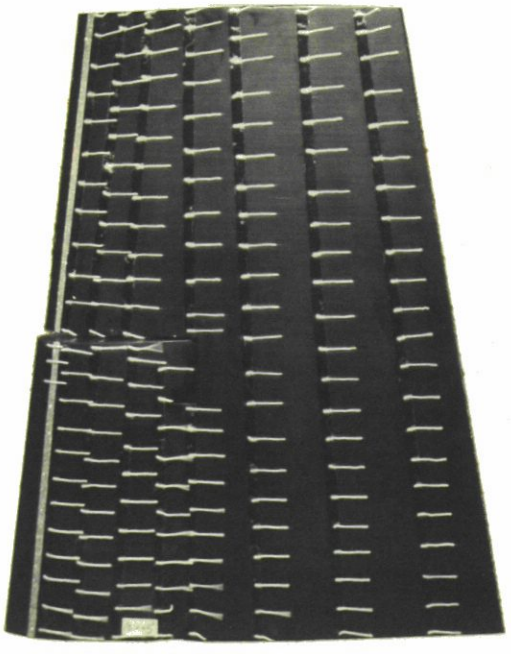

$\beta = +5°$
$\delta = -15°$ $(\alpha = -10°)$

$\beta = -5°$
$\delta = +20°$ $(\alpha = 15°)$

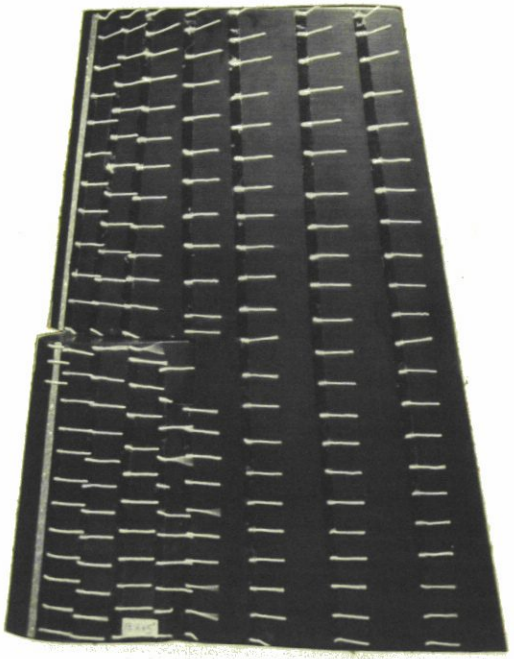

$\beta = +5°$
$\delta = -20°$ $(\alpha = -15°)$

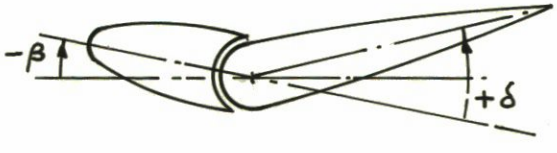

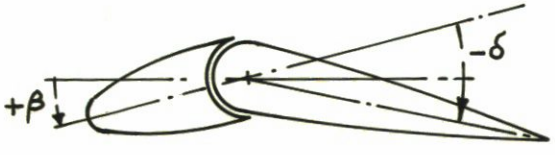

Fig. 12b FLOW PATTERNS OVER RUDDER

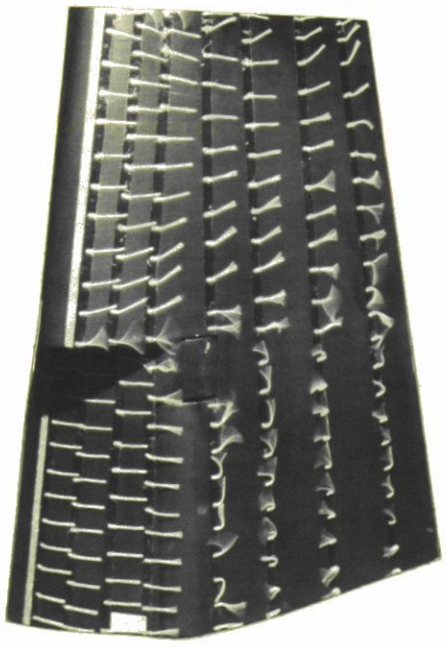

$\beta = -5°$
$\delta = +30°$ ($\alpha = 25°$)

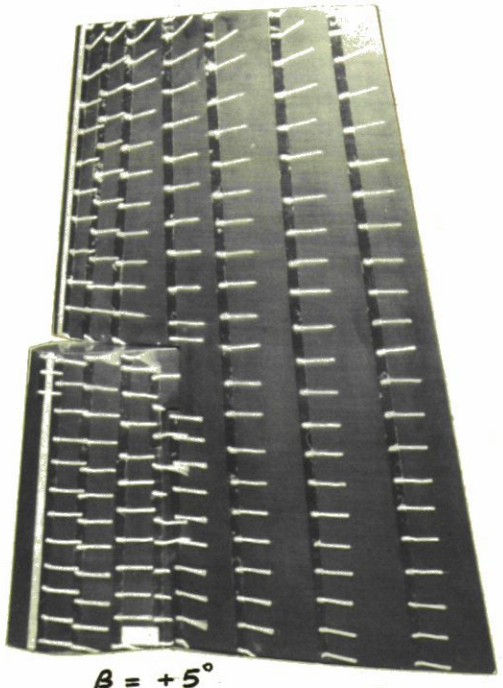

$\beta = +5°$
$\delta = -30°$ ($\alpha = -25°$)

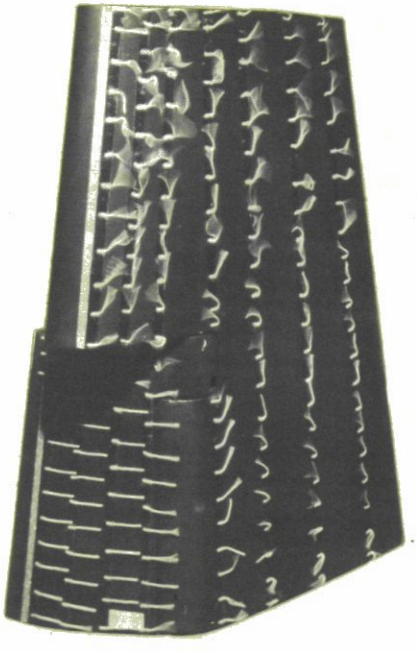

$\beta = -5°$
$\delta = +40°$ ($\alpha = 35°$)

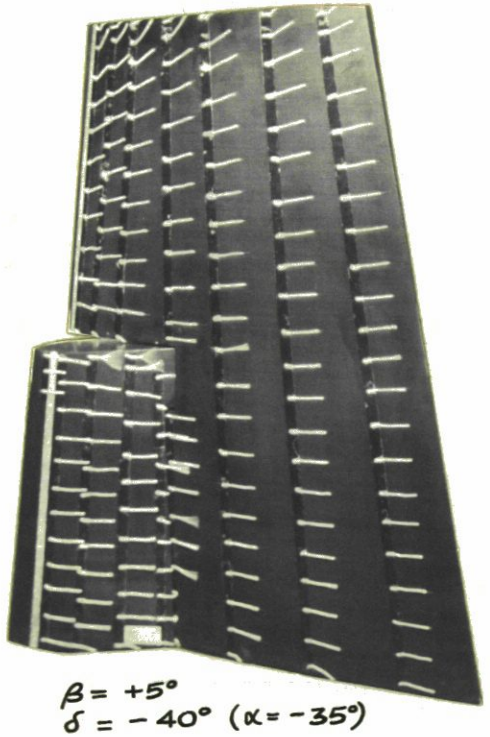

$\beta = +5°$
$\delta = -40°$ ($\alpha = -35°$)

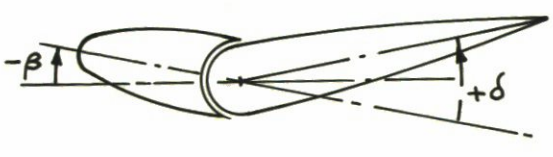

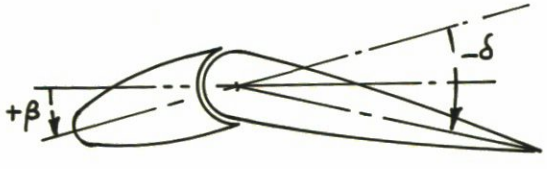

Fig. 12c FLOW PATTERNS OVER RUDDER